

**UNIVERSITY OF GAZIANTEP
GRADUATE SCHOOL OF
NATURAL & APPLIED SCIENCES**

**GENETIC PROGRAMMING
BASED MODELING OF
TORSIONAL STRENGTH OF RC BEAMS**

**M. Sc. THESIS
IN
CIVIL ENGINEERING**

**BY
PINAR KORKMAZ
AUGUST 2011**

**Genetic Programming Based Modeling of Torsional
Strength of RC beams**

**M.Sc. Thesis
in
Civil Engineering
University of Gaziantep**

**Supervisor
Assoc. Prof. Dr. Abdulkadir ÇEVİK**

**by
Pınar Korkmaz
August 2011**

T.C.
UNIVERSITY OF GAZİANTEP
GRADUATE SCHOOL OF
NATURAL & APPLIED SCIENCES
NAME OF THE DEPARTMENT

Name of the thesis: Genetic Programming Based Modeling Of Torsional Strength Of
RC Beams

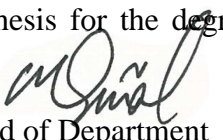
Name of the student: Pınar Korkmaz

Exam date: August 2011

Approval of the Graduate School of Natural and Applied Sciences


Director
Prof. Dr. Ramazan KOÇ

I certify that this thesis satisfies all the requirements as a thesis for the degree of
Master of Science/Doctor of Philosophy.


Head of Department
Assoc. Prof. Dr. Mustafa GÜNAL

This is to certify that we have read this thesis and that in our consensus/majority
opinion it is fully adequate, in scope and quality, as a thesis for the degree of Master
of Science/Doctor of Philosophy.

Supervisor
Assoc. Prof. Dr. Abdulkadir ÇEVİK


signature

Examining Committee Members

Title and Name-surname

Prof. Dr. Mustafa ÖZAKÇA

Assoc. Prof. Dr. Abdulkadir ÇEVİK

Asst. Prof. Dr. Nihat ATMACA


Three horizontal lines with handwritten signatures in blue ink above them.

ABSTRACT

GENETIC PROGRAMMING BASED MODELING OF TORSIONAL STRENGTH OF RC BEAMS

KORKMAZ, Pınar

M.Sc. in Civil Eng.

Supervisor: Assoc. Prof.Dr. Abdulkadir ÇEVİK

August 2011,87 Pages

This study presents the application of Genetic Programming (GP) for modeling torsional strength of RC beams. In the literature, experimental data of 76 rectangular RC beams from an existing database were used to develop the GP model. The input parameters affecting the torsional strength were selected as cross-sectional area of beams, dimensions of closed stirrups, spacing of stirrups, cross-sectional area of one-leg of closed stirrup, yield strength of stirrup and longitudinal reinforcement, steel ratio of stirrups, steel ratio of longitudinal reinforcement and concrete compressive strength. Besides, the building codes in relation to the design of RC beams under pure torsion is presented. The accuracy of the codes in predicting the torsional strength of RC beams was also compared with the proposed GP model with comparable way by using same test data. The study concludes that the proposed GP model predicts the torsional strength of RC beams by far more accurate than building codes.

Key Words: Reinforced concrete beam, Genetic Programming, Torsional strength, Building code.

ÖZET

BETONARME KİRİŞLERİN BURULMA DAYANIMININ GENETİK PROGRAMLAMA İLE MODELLENMESİ

KORKMAZ, Pınar

Yüksek Lisans Tezi, İnş Müh. Bölümü

Tez Yöneticisi: Doç. Dr. Abdulkadir ÇEVİK

Ağustos 2011,87 sayfa

Bu çalışmada betonarme kirişlerin burulma dayanımının Genetik Programlama (GP) ile modellenmesi sunulmuştur. Literatürden mevcut bir veritabanına ait 76 dikdörtgen betonarme kirişin deneysel verileri GP modeli geliştirmek için kullanılmıştır. Burulma dayanımını etkileyen girdi parametreleri kirişlerin kesit alanı, kapalı etriye boyutları, etriye aralığı, tek ayak kapalı etriye kesit alanı, etriye akma dayanımı ve boyuna donatı, etriye çelik oranı, boyuna donatı çelik alanı ve beton basınç dayanımı olarak seçilmiştir. Ayrıca, burulma altındaki betonarme kirişlerin dizaynı ile ilgili olarak bina kodları sunulmuştur. Betonarme kirişlerin burulma dayanımını belirlemek için geliştirilmiş kodların doğruluğu aynı test verilerinin kullanılması ile önerilen Genetik Programlama modelinden istifade edilerek karşılaştırılmıştır. Bu karşılaştırma sonucu göstermiştir ki; önerilen Genetik Programlama modeli, betonarme kirişlerin burulma dayanımını diğer kodlara kıyasla çok daha doğru hassasiyet ile belirlemektedir.

Anahtar Kelimeler: Betonarme Kirişler, Genetik Programlama, Burulma dayanımı, Bina kodu.

ACKNOWLEDGMENTS

I would like to express my deepest gratitude to my supervisor Assoc. Prof. Dr. Abdulkadir Çevik for his continuous support, guidance and encouragement throughout the course of my study and research.

I would also like to thank my friend Bilgen Çeliktürk for her support.

Most of all, I would like to thank my mother, my father and my brother. They always provided heartfelt support and encouraged me.

CONTENTS	page
ABSTRACT	iii
ACKNOWLEDGMENTS	v
CONTENTS	vi
LIST OF TABLES	viii
LIST OF FIGURES	ix
LIST OF SYMBOLS	xi
CHAPTER 1 : INTRODUCTION	1
1.1 GENERAL INTRODUCTION	1
1.2 LAYOUT OF THE THESIS	2
CHAPTER 2 : LITERATURE REVIEW	3
2.1 ENGINEERING ANALYSIS	3
2.2 RC BEAMS	3
2.2.1 ADVANTAGES OF USING HIGH STRENGTH CONCRETE	4
2.3 GENETIC PROGRAMMING	5
2.3.1 GENETIC PROGRAMMING IN STRUCTURAL MECHANICS	5
CHAPTER 3 : TORSIONAL STRENGTH OF RC BEAMS	6
3.1 TORSIONAL STRENGTH	6
3.1.1 TORSION – COMBINED TORSION, SHEAR AND FLEXURE	6
3.1.2 THEORIES OF TORSIONAL STRENGTH AND TORSION IN THE BUILDING STANDARDS	9
3.1.3 PURE TORSION	14
3.1.4 TORSION IN ELASTIC MATERIALS	18
3.1.5 TORSION IN PLASTIC MATERIALS	20
3.1.6 SAND-HEAP ANALOGY APPLIED TO L BEAMS	20
3.1.7 SKEW-BENDING THEORY	25
3.1.8 TORSION IN REINFORCED CONCRETE ELEMENTS	29

3.1.9 SPACE TRUSS ANALOGY THEORY	30
3.1.10 EQUILIBRIUM IN ELEMENT SHEAR	33
3.1.11 EQUILIBRIUM IN ELEMENT TORSION	35
3.1.12 SHEAR-TORSION-BENDING INTERACTION	36
3.2 ACI DESIGN OF REINFORCED CONCRETE BEAMS SUBJECTED TO COMBINED TORSION BENDING AND SHEAR.....	38
3.2.1 TORSIONAL BEHAVIOR OF STRUCTURES	38
3.2.2 TORSIONAL MOMENT STRENGTH	40
CHAPTER 4 : GENETIC PROGRAMMING	41
4.1 GENETIC PROGRAMMING SYSTEMS	41
4.1.1 GENETIC PROGRAMMING	41
4.1.2 SOLVING A SIMPLE PROBLEM WITH GEP	43
CHAPTER 5 : NUMERICAL APPLICATION	48
5.1 NUMERICAL APPLICATION	48
5.2 DISCUSSIONS	58
5.2.1 CODE APPROACHES	58
5.2.2 GENETIC PROGRAMMING (GP)	59
5.3 MAIN EFFECTS OF VARIABLES ON TORSIONAL STRENGTH	60
CHAPTER 6 : CONCLUSION.....	73
6.1 CONCLUSION	73
APPENDIX	74
REFERENCES.....	81

LIST OF TABLES

	page
Table 5.1 Ranges of variables of the database	49
Table 5.2 Parameters of GP models	50
Table 5.3 Statistical parameters of the proposed GP models	51
Table 5.4 Prediction accuracy of existing building codes	52
Table A1. Experimental database [Rasmussen and Baker (1995), Koutchoukali and Belarbi (2001), Fang and Shiau (2004), Hsu(1968)	74
Table A2. Trainig and testing results	78

LIST OF FIGURES

	page
Figure 3.1 Shear stress	7
Figure 3.2 Torsional moment	7
Figure 3.3 Torque	8
Figure 3.4 Skew-bending theory analogy	10
Figure 3.5 Thin-walled tube and space-truss analogy	11
Figure 3.6 The cross section of a rectangular reinforced concrete beam	13
Figure 3.7 Torsional stress distribution through circular section	15
Figure 3.8 Pure torsion stress distribution in a rectangular section	15
Figure 3.9 Plain concrete beam	16
Figure 3.10 Reinforced beams	17
Figure 3.11 Membrane analogy in elastic pure torsion	19
Figure 3.12 Sand-heap analogy in plastic pure torsion	21
Figure 3.13 Sand-heap analogy of flanged section	23
Figure 3.14 Skew bending due to torsion	27
Figure 3.15 Forces on the skewly bent planes	28
Figure 3.16 Space truss model	31
Figure 3.17 Forces on hollow box concrete surface by truss analogy	33
Figure 3.18 Equilibrium forces in element shear	34
Figure 3.19 Hollow tube equilibrium torsion forces	35
Figure 3.20 Shear-torsion interaction diagram	37
Figure 4.1 Expression tree for the problem of eqn.4.1	46
Figure 4.2 Gene expression programming flowchart	47
Figure 5.1 Performance of test and GP results	53

Figure 5.2 Expression tree for torsional strength of RC beams	55
Figure 5.3 Main effect plot for T_u	61
Figure 5.4 Interaction plot for T_u	62
Figure 5.5 Surface plot of T_u vs $A_c, A_L f_{yL}$	63
Figure 5.6 Surface plot of T_u vs $A_c, A_t f_{yt}/s$	64
Figure 5.7 Surface plot of T_u vs A_c, f_c	65
Figure 5.8 Surface plot of T_u vs A_c, P_c	66
Figure 5.9 Surface plot of T_u vs $A_L f_{yL}, P_c$	67
Figure 5.10 Surface plot of T_u vs $A_L f_{yL}, f_c$	68
Figure 5.11 Surface plot of T_u vs $A_L f_{yL}, A_t f_{yt}/s$	69
Figure 5.12 Surface plot of T_u vs $A_t f_{yt}/s, f_c$	70
Figure 5.13 Surface plot of T_u vs $A_t f_{yt}/s, P_c$	71
Figure 5.14 Surface plot of T_u vs f_c, P_c	72

LIST OF SYMBOLS

A	: total area
A_o	: gross area enclosed by the shear flow path
A_e	: area enclosed by lines connecting the centroids of the reinforcing bars at the corner of the section
A_k	: area enclosed by the centre-lines of the effective wall thickness
A_ℓ	: total area of longitudinal torsional reinforcement
A_{sh}	: area enclosed by the centre of stirrups
A_{sv}	: area of the two legs of stirrups at a section ($=2A_t$)
A_t	: cross sectional area of one-leg of closed stirrup
a_i	: outputs of neural network
f_c	: compressive strength of concrete
$f_{y\ell}$: yield strength of longitudinal torsional reinforcement
f_{yv}	: yield strength of closed stirrups
k	: number of samples in training or test data
m	: number of segments in training or test data
n	: number of outputs of neural network for training and test procedures
ρ_ℓ	: steel ratio of longitudinal reinforcement
ρ_t	: steel ratio of stirrups
ρ_h	: perimeter of centerline of outmost closed transverse torsional reinforcement

R^2	: correlation coefficient
s	: spacing of stirrups
s_x	: normalized value of variable
T_c	: torsion moment resisted by the concrete compression struts
T_n	: nominal torsional strength
$T_{u(\text{estimated})}$: predicted ultimate torsional strength
$T_{u(\text{experimental})}$: measured ultimate torsional strength
t_{ef}	: the effective wall thickness
t_i	: desired outputs
u	: perimeter of the cross-section
x	: short dimension of the cross section
y	: long dimension of the cross section
x_1	: center-to-center of the shorter and longer legs of stirrups
y_1	: center-to-center of the longer legs of stirrups
z	: variable values
z_{\min}	: variable minimum values
z_{\max}	: variable maximum values
θ	: angle of compression diagonals

CHAPTER 1

INTRODUCTION

1.1 General Introduction

The monolithic reinforced concrete constructions are subjected to significant torsional moments that affect their strength and deformation. In the literature, numerous analytical and experimental studies have been reported about torsional behavior of reinforced concrete (RC) members which subjected to pure tension or combination of tension with other effects as axial load, shear and bending.

There are many variables affecting the torsional strength of RC beams such as cross-sectional area of beams, dimensions of closed stirrup, spacing of stirrups, cross-sectional area of one-leg of closed stirrup, yield strength of stirrup and longitudinal reinforcement and concrete compressive strength. The effect of these variables on the torsional strength of RC beams has been extensively studied and some empirical approach has been developed related to variables.

Test data are often used for validation, calibration or even development of models. Even though the torsional strength of RC beams has been carefully examined experimentally, estimation of torsional strength is still difficult task because of complex behavior of RC beam under torsional action.

The main aim of this study is to investigate the applicability of Genetic Programming (GP) to propose a new model for the torsional strength of RC beams based on experimental results collected from the literature and to evaluate the accuracy of the building codes in predicting the ultimate torsional strength of RC beams. In this sense, experimental data of 76 beams subjected to torsion were used from existing databases of Rasmussen and Baker (1995) , Koutchoukali and Belarbi

(2001), Fang & Shiau (2004), Hsu (1968). Furthermore, some building code' approaches as ACI-318-2005 (ACI,2005) , Eurocode-2 (2002), TBC-500-2000 (TBC,2000), CSA (1994), BS8110 (1985) and AS3600 (2001) are also examined by comparing their predictions with mentioned experimental studies results. The results obtained by the proposed GP model and building codes are compared with each other. (Çevik et al.,2009)

1.2 Layout of the Thesis

The layout of the thesis is described below:

- Chapter 1 is a general introduction about the thesis.
- Chapter 2 is the literature survey for torsional strength of reinforced concrete beams and is summarized genetic programming.
- Chapter 3 is devoted to the torsional strength of RC beams. The basic theory and torsional strength formula of RC beams presented and several Building Codes examples are studied.
- Chapter 4 is presents gene expression programming, its system, and solutions of GP are summarized.
- Chapter 5 deals with statistical parameters of testing and training sets and overall results of GP models and experimental results of GP models.
- Finally in Chapter 6 brief conclusions are presented together.

CHAPTER 2

LITERATURE REVIEW

2.1 Engineering Analysis

Engineering analysis involves the application of scientific analytic principles and processes to reveal the properties and state of the system, device or mechanism under study. The purpose of any engineering analysis is to predict the behavior of an engineering system under specified conditions. In other words: given the input to the system what is the output from the system? The engineering system under analysis could be, for example, a simple elastic beam, a complex nonlinear three-dimensional structure, mechanical equipment or a hydraulic network. Engineering analysis is the process of taking given "input" information defining the physical situation at hand and, through an appropriate set of *manipulations*, converting that input into a different form of information, the "output," which provides the answer to some questions of interest (Gallegher,1995).

2.2 RC Beams

Experimental and theoretical studies on shear strength of large reinforced concrete beams are presented. In the literature various approaches are available for the determination of the ultimate torsional strength of reinforced concrete beams. The space truss theory (Rausch,1929) is overconservative specially for underreinforced sections (Hsu, 1968) whereas the skew bending model (Lessig,1953); (Yudin,1962) appears to better predict the observed results, but is cumbersome to use and sometimes can be overconservative. An interesting limit analysis method to find the ultimate torsional strength of reinforced concrete members was proposed by Wang and Hsu (1997), in which the work equation based upon the energy dissipation rate and the permissible failure mechanism at the

ultimate state was used. This method gives good estimates of the experimental results reported by Hsu(1968). Taking a clue from their earlier work Phatak and Dhonde (1999), the writers have formulated a general equation to determine the ultimate torsional strength of reinforced concrete beams using a unique method of dimensional analysis. The results predicted by dimensional analysis are then compared with the experimental results (Hsu, 1968) and the limit analysis method Wang and Hsu (1997).

2.2.1 Advantages of Using High Strength Concrete

High-strength concrete is one of the most significant new materials available to federal, state, and local highway agencies. With its improved impermeability, durability, and accelerated strength gain, an ideal material. There are many advantages of high strength concrete. The following list provides some of them.

- Reduction in member size, resulting in (a) increase in rentable space and (b) reduction in the volume of produced concrete with the accompanying saving in construction time.
- Reduction in the self-weight and superimposed dead load with the accompanying saving in smaller foundations.
- Reduction in formwork area and cost with the accompanying reduction in shoring and stripping time due to high early-age gain in strength.
- Construction of higher high-rise buildings with the accompanying saving in real estate costs in congested areas.
- Longer spans and fewer beams of the same magnitude of loading.
- Reduced axial shortening of compression supporting members.
- Reduction in the number of supports and the supporting foundations due to the increase in spans.
- Reduction in the thickness of floor slabs and supporting beam sections (a major component of the weight and cost of the majority of structures).
- Superior long-term service performance under static, dynamic, and fatigue loading.
- Low creep and shrinkage.

- Greater stiffness as a result of a higher modulus, E_c .
- Higher resistance to freezing and thawing, chemical attack, and significantly improved long-term durability and crack propagation

2.3 Genetic Programming

Genetic programming (GP) is a systematic, domain-independent method for getting computers to solve problems automatically starting from a high-level statement of what needs to be done. Using ideas from natural evolution, GP starts from an ooze of random computer programs, and progressively refines them through processes of mutation and sexual recombination, until solutions emerge. All this without the user having to know or specify the form or structure of solutions in advance. GP has generated a plethora of human-competitive results and applications, including novel scientific discoveries and patentable inventions.(<http://www.gp-field-guide.org.uk/>)

2.3.1 Genetic Programming in Structural Mechanics

The application of Genetic programming to civil engineering design problems in structural mechanics is relatively new. GP can be applied to structural design problems to produce solutions that offer significant improvements over traditional GA based methods.

GPs automatically generate computer programs. The theory states that there is no need to know anything about the problem one is trying to solve, as long as there is a “black box” which evaluates the solutions proposed. However, in practice the use of these methods should not be a substitute for thought, since taking into account of problem specific knowledge can considerably improve the effectiveness of this methodology.

The best computer program that appears in any generation (i.e. best so far individual) is designed as the result of GP. This result may be a solution or an approximate solution to the problem.(Yan W.,2003)

CHAPTER 3

TORSIONAL STRENGTH OF

REINFORCED CONCRETE BEAMS

3.1 Torsional Strength

3.1.1 Torsion – Combined Torsion, Shear and Flexure

Due to the monolithic nature of concrete construction, a great many of the structural members are subjected to torsion. However in many cases these torsional moments are of negligible magnitude. Torsional moments are created either by geometry or due to the unsymmetrical arrangement of live loads. It is very difficult to calculate the torsional moments carried by reinforced concrete members due to inelastic behavior of concrete and due to complex boundary conditions. Torsional moments calculated using a linearly analysis are usually unrealistically high. (Ersoy et al.,2003)

Torsional moments produce shear stresses. These shear stresses are in opposite directions on opposite faces of the member. If the member is subjected to flexural shear in addition to torsion, the torsional shear stresses are additive to flexural shear stresses on one face of the member. On the opposite face, these two types of shear stresses are in opposite directions. Torsional shear stresses, which are additive to the flexural shear stresses on one face of the member, obviously increase the principal tensile stresses. Since concrete is very weak in tension, principal tensile stresses are of great importance. Shear stresses produced by torsion and flexural shear and resulting principal tension are shown in Figure 3.1. (Ersoy et al.,2003)

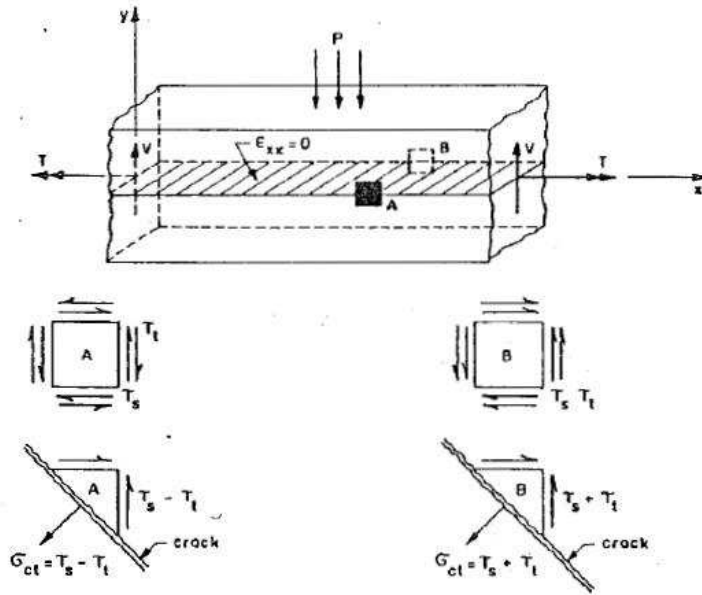


Figure 3.1 Shear Stress (Ersoy et al.,2003)

The presence of torsional moments in structural floor systems is illustrated in Figure 3.2. Such torsional moments exist even when the adjacent slabs have equal spans, due to checker board arrangement of live loads. However torsional moments created in such cases are usually very small. In this case distribution of torsional moments along the span will be as shown on the figure. (Ersoy et al.,2003)

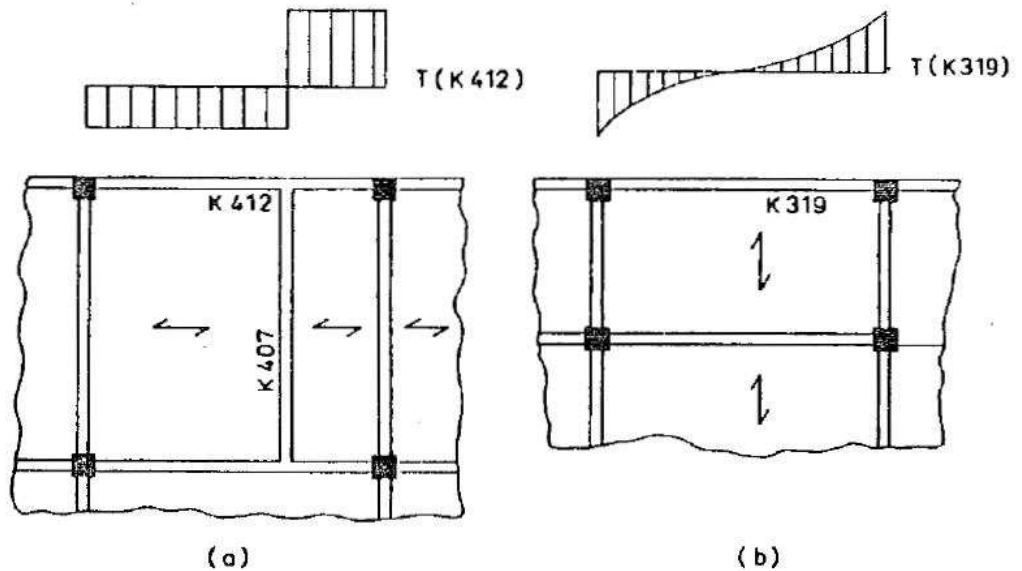


Figure 3.2 Torsional Moment(Ersoy et al.,2003)

Torsional shear stresses calculated using torsional moments obtained from linearly elastic analyses were usually very high. In Figure 3.3(a), very high torsional

moments were produced at one end of girder. Diagonal cracks on opposite faces were almost orthogonal to each other. As is illustrated in Figure 3.2, this type of diagonal cracking is very typical when torsion is dominant. (Ersoy et al.,2003)

In the second case, partial floor plan shown in Figure 3.3(b), severe flexural cracking was observed on the top of the slab, almost parallel to girder. An analysis of this floor system indicated that these slab cracks were caused by the torque applied by beams. The applied torque had to be shared by girder as torsional moments and by the slab as flexural moments. This is illustrated on the free body shown in Figure 3.3(b). The difference in torque between the two faces of the girder (ΔT) has to be equal to the moments created in the slab

$$\Delta T = \Sigma m \tag{3.1}$$

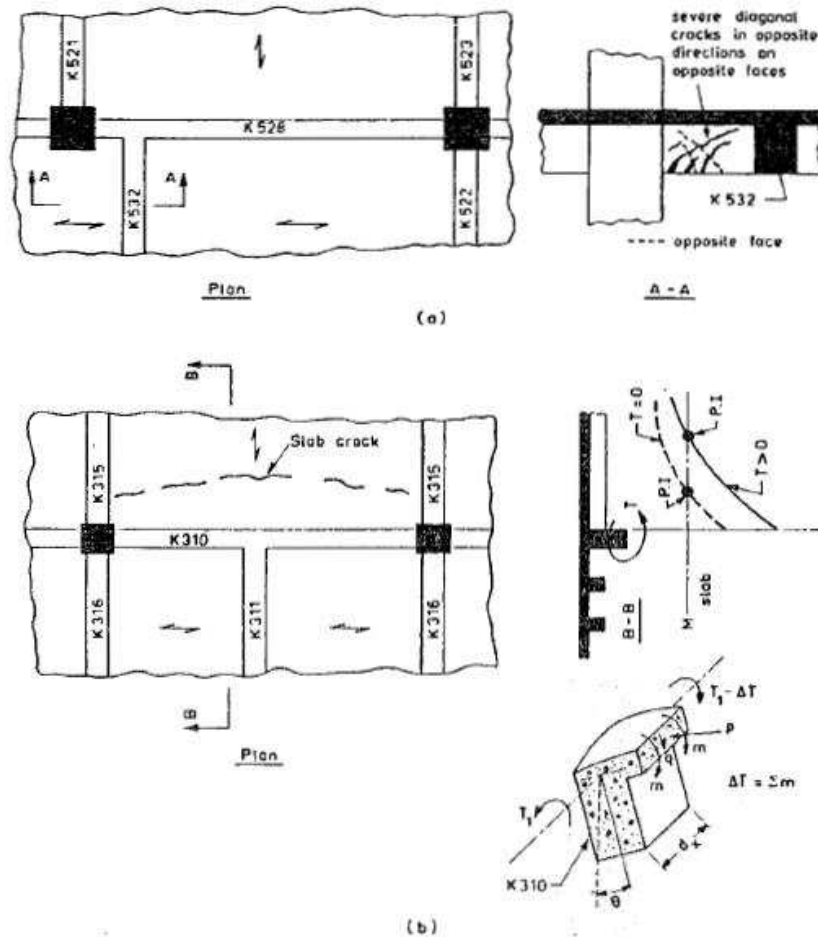


Figure 3.3 Torque (Ersoy et al.,2003)

The extra negative moments created in the slab due to the applied torque pushed the point of inflection away from the girder as shown in Figure 3.3(b) Since the slab was designed without considering the influence of the applied torque (in accordance with the moment diagram shown by the dotted line), top steel was cut close to girder. Since the point of inflection moved away from the girder due the applied torque, negative moments were produced in regions where there was no top steel. Therefore opening of cracks could not be prevented.(Ersoy et al.,2003)

3.1.2. Theories of Torsional Strength and Torsion in the Building Standards

Several theories have been proposed for the computation of the torsional strength of reinforced concrete members with torsional reinforcement—notably the space-truss analogy and the skew bending theory. In this section, the two theories for torsional strength of reinforced concrete members are reviewed briefly. On the other hand, the ACI Building Code provisions for torsional design were selected and used in this study for comparison with the results from the RBFN models. Therefore, the ACI equations for torsional strength of RC beams are also outlined in the following. (Nawy,2003)

In 1958, the skew-bending theory which considers in detail the internal deformational behavior of the series of transverse warped surfaces along the beam was proposed by Lessig (Lessig,1959). The model was further refined by Collins (Collins et al.,1965) in 1965 as well as Hsu and Zia (Hsu,1968, Zia and Hsu, 2004). Especially Hsu made a major contribution experimentally to the development of the skew-bending theory as it presently stands. The basic approach of the theory is that the failure of a rectangular section in torsion occurs by bending about an axis which is parallel to wider face of the section and inclined at about 45° to the longitudinal axis of the beam. In previous versions of ACI code (from 1971 to 1989) (ACI Committee), torsional strength of beams was calculated by using this theory. (Nawy,2003)

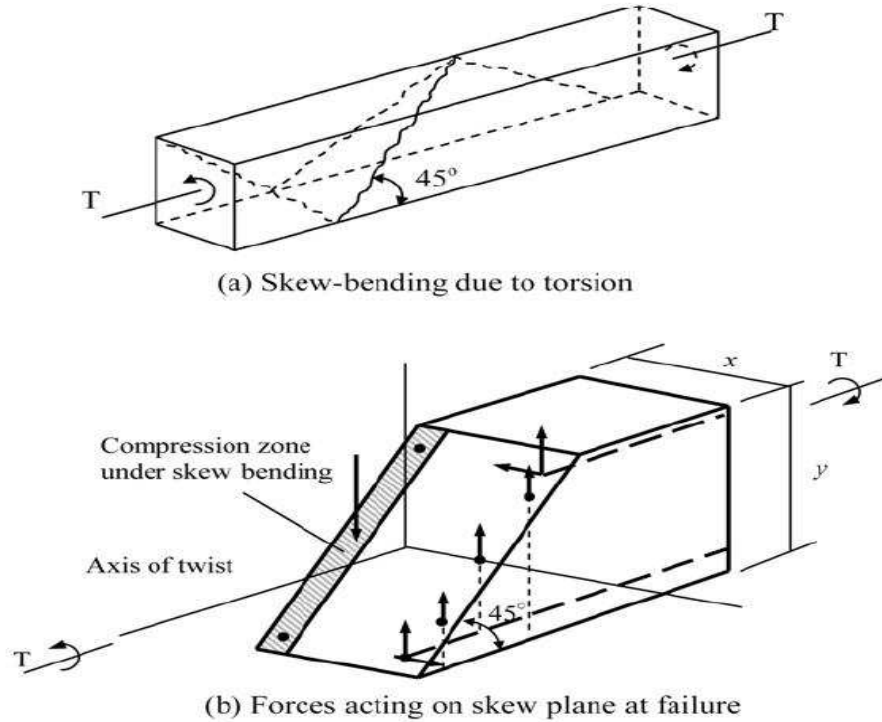


Figure 3.4 Skew-bending theory analogy (Tang, 2006)

According to the codes, torsional strength T_n of beams was considered to be made up of two parts: one part is contributed by concrete T_c while the other part is contributed by web reinforcement T_s . Hsu on hollow and solid rectangular beams, it was observed that the concrete core does not contribute to the ultimate torsional strength. Later he concluded that the concrete contribution T_c was mainly due to the shear resistance of the diagonal concrete struts. (Hsu,1968).

In the space truss model the torsion is resisted by compression diagonals that consist of the concrete between cracks that spiral around the beam at a constant angle. The theory has been extended later by many scholars in this field (Hsu,1968), (Elfgren et al.,1974). It is assumed in this theory that the concrete beam behaves in torsion similar to a thin-walled box with a constant shear flow in the wall cross-section, producing a constant torsional moment (Nawy,2003). The absence of core does not affect the strength of such members in torsion; hence the acceptability of the space truss analogy approach based on hollow sections. Therefore, in the process of

torsion design of a RC beam, the beam can be considered to be equivalent tubular member (Çevik et al.,2010).

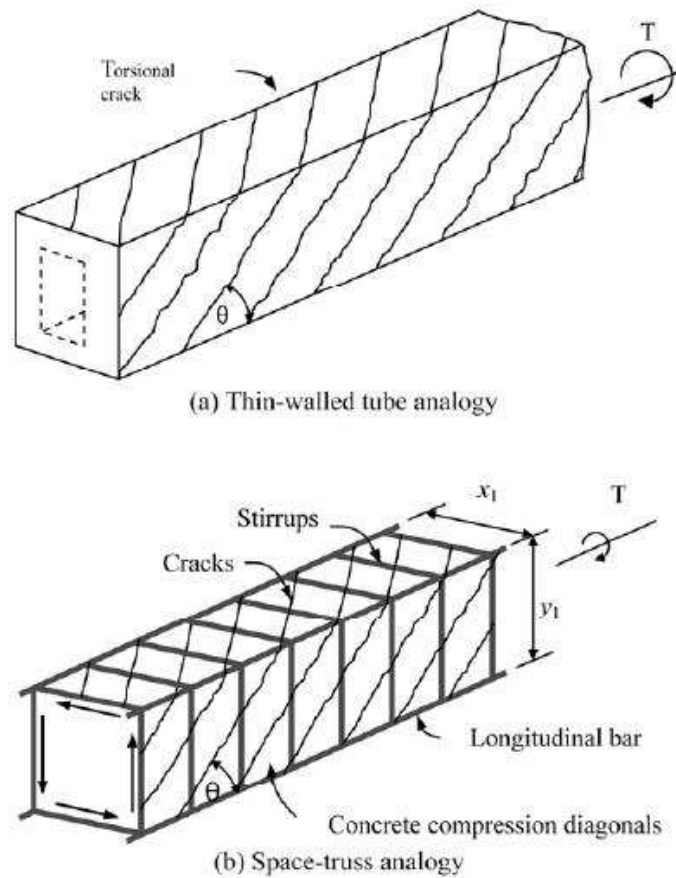


Figure 3.5 Thin-walled tube and space-truss analogy (Tang, 2006)

ACI code was proposed a radically different design procedure based on the thin-walled tube, space truss analogy which is considerably simpler to understand and apply and is equally accurate. The torsion provisions in the ACI 318 have been revised using the thin walled tube analogy (ACI,1995).

According to the current torsion provision of ACI 318-2005 (ACI, 2005), meaningful additional torsional strength T_n of RC beams can be achieved only by using both closed stirrups and longitudinal steel bars while the torsion moment T_c resisted by the concrete compression struts is assumed as zero. Thus the concrete contribution is ignored; there is no advantage in using higher concrete strengths in resisting ultimate torsion. The torsional strength T_n is given as follows;

$$T_n = \frac{2A_o A_t f_{yv}}{s} \cot \theta \quad (3.2)$$

In the Eq.3.2, $\cot \theta$ can be assumed as

$$\cot \theta = \sqrt{\frac{A_\ell f_{y\ell} s}{A_t f_{yv} p_h}} \quad (3.3)$$

In the equation 3.2 and 3.3, A_o is the gross area enclosed by the shear flow path that can be equal to $0.85 A_{sh}$, where A_{sh} is the area enclosed by the centre of stirrups. θ angle of compression diagonals, $f_{y\ell}$ yield strength of longitudinal torsional reinforcement, f_{yv} is yield strength of closed stirrups, A_ℓ total area of longitudinal torsional reinforcement, p_h perimeter of centerline of outmost closed transverse torsional reinforcement, s spacing of stirrups, A_t cross sectional area of one-leg of closed stirrup (Çevik et al.,2010).

In Australian Standard AS3600 (2001) and Canadian Standard CSA,(1994) the design of RC beams subjected to pure torsion is based on the space truss model and the T_n value is given as the same equation with ACI-318-2005 (2002). Different from ACI 318-2005 (1995), CSA (1994) and AS3600 (2001), The British Standards BS8110 (1985) for RC structures, the torsional strength shall be calculated from Equation 3.4 as;

$$T_n = \frac{0.8x_1 y_1 (0.87f_{ys}) A_{sv}}{s} \quad (3.4)$$

where A_{sv} is the area of the two legs of stirrups at a section and x_1 and y_1 are the center-to-center of the shorter and longer legs of stirrups given in Figure 3.5. The

torsional strength T_n is described as Equation 3.5 in Turkish Building Code TBC-500-2000.

$$T_n = \frac{2A_\ell A_e f_{yv}}{2(x_1 + y_1)} \quad (3.5)$$

In the Equation 3.5, A_e is area enclosed by lines connecting the centroids of the reinforcing bars at the corner of the section as seen in Figure 3.6.

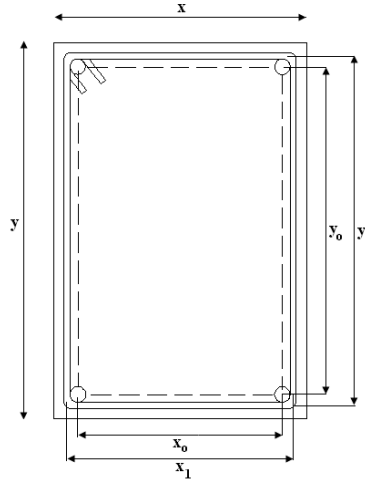


Figure 3.6 The cross section of a rectangular reinforced concrete beam (Çevik et al.,2010).

According to the European Standard Eurocode-2 (2002), torsional strength shall be calculated with three ways and the minimum result is chosen.

$$T_n = f_{ys} (A_{sw} / s) 2A_k \cot \theta \quad (3.6)$$

$$T_n = f_y (A_s / u_k) 2A_k \tan \theta \quad (3.7)$$

$$T_n = 1.2(1 - f_c / 250) f_c A_k t_{ef} \sin \theta \cos \theta \quad (3.8)$$

Where A_k is the area enclosed by the centre-lines of the effective wall thickness. The effective wall thickness, t_{ef} can be calculated as A/u where A is the total area and u is the perimeter of the cross-section, f_c is the compressive strength of concrete (Çevik et al.,2010).

3.1.3 Pure Torsion

In practice pure torsion is extremely rare. Due to the monolithic nature of concrete construction, flexural moments, shear and axial forces are present in addition to torsion (Ersoy et al.,2003).

An introduction to the subject of torsional stress distribution has to start with the basic elastic behavior of simple sections, such as circular or rectangular sections. Most concrete beams subjected to twist are components of rectangles. They are usually flanged sections such as T beams and L beams. (Nawy,2005).

Although circular sections are rarely a consideration in normal concrete construction, a brief discussion of torsion in circular sections serves as a good introduction to the torsional behavior of other types of sections. Shear stress is equal to shear strain times the shear modulus at the elastic level in circular sections. As in the case of flexure, the stress is proportional to its distance from the neutral axis and is maximum at the extreme fibers. When deformation takes place in the circular shell, the axis of the circular cylinder is assumed to remain straight. All radii in a cross-section also remain straight and rotate through the same angle about the axis. As the circular element starts to behave plastically, the stress in the plastic outer ring becomes constant while the stress in the inner core remains elastic, as shown in Figure 3.7. (Nawy,2005).

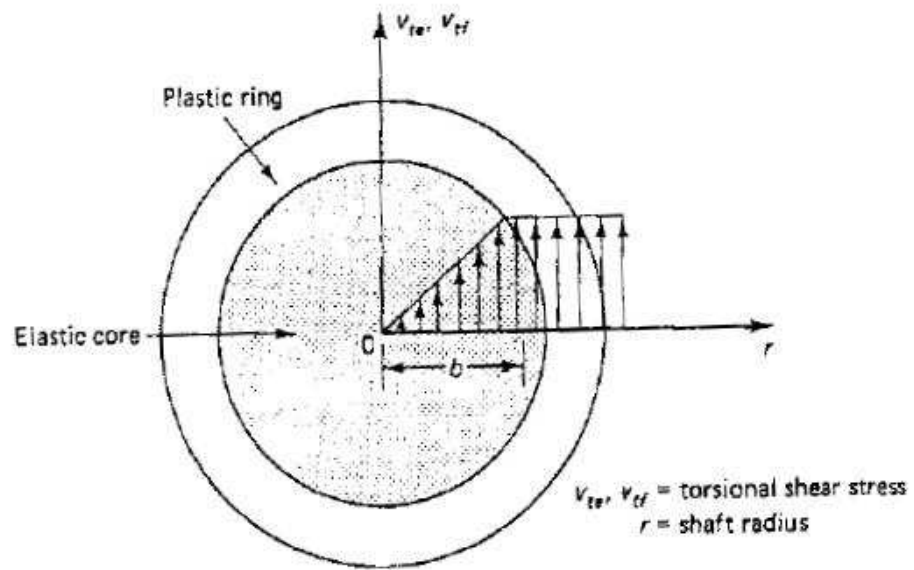


Figure 3.7 Torsional stress distribution through circular section (Nawy,2005).

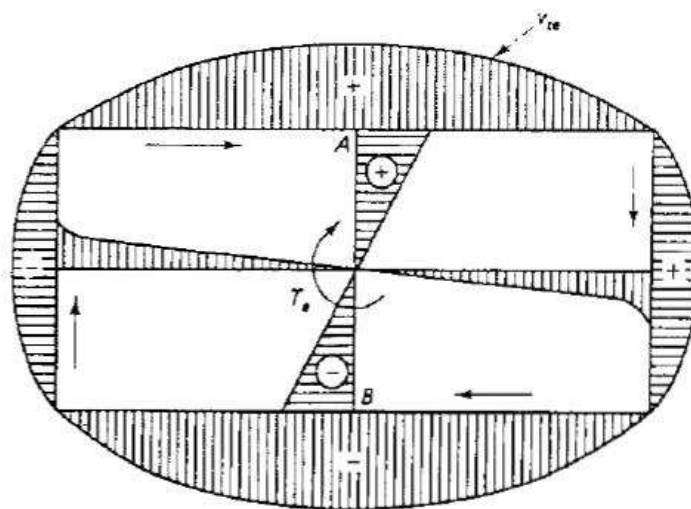


Figure 3.8 Pure torsion stress distribution in a rectangular section (Nawy,2005).

In rectangular sections, the torsional problem is considerably more complicated. The originally plane cross sections undergo warping due to the applied torsional moment. This moment produces axial as well as circumferential shear stresses with zero values at the corners of the section and the centroid of the

rectangle and maximum values on the periphery at the middle of the sides, as seen in Figure 3.8. The maximum torsional shearing stress would occur at midpoints A and B of the larger dimension of the cross-section. These complications plus the fact that reinforced concrete sections are neither homogeneous nor isotropic make it difficult to develop exact mathematical formulations based on physical models (Nawy,2005).

A plain concrete beam, having convex cross-sections, (such as rectangular section) subjected to pure torsion fails upon the formation of the first inclined crack. The failure is sudden and brittle. The failure crack is approximately orthogonal to the direction of principal tensile stresses on three faces of the beam as would be predicted by the theory of elasticity. However on the fourth face (longer side of the rectangle), the crack direction is opposite to expected direction. If carefully examined, it will be observed that this is not really a crack, but a line along which concrete has crushed. The crack pattern is shown in Figure 3.9. (Ersoy et al.,2003)

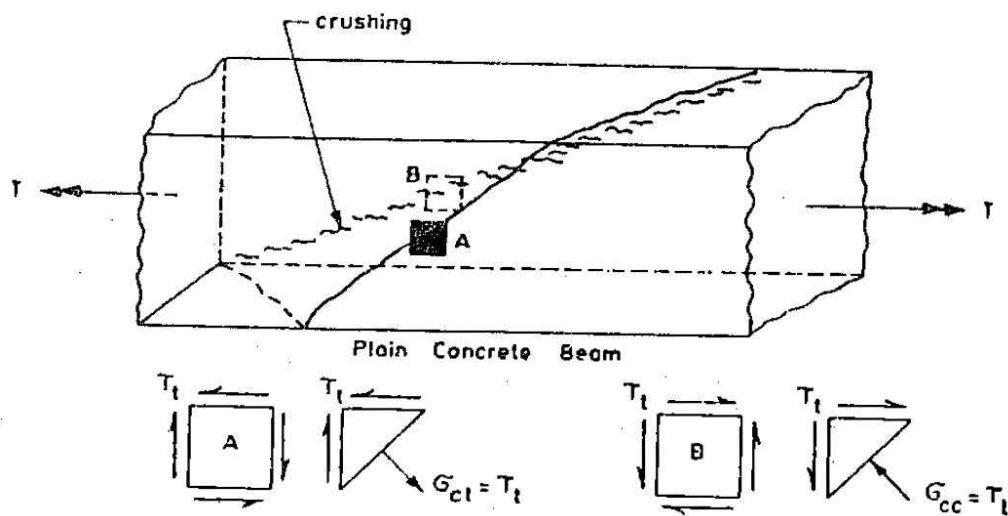


Figure 3.9 Plain Concrete Beam (Ersoy et al.,2003)

Plain concrete beams with concave sections (like T and L shapes) behave similar to beams with convex sections up to the first cracking. First cracks are usually observed on the web almost orthogonal to the direction of principal tensile stresses. Cracks on opposite faces are orthogonal to each other as would be predicted by the theory of elasticity. Beams with concave cross-sections do not fail upon the

formation of the first crack, but continue to carry the increasing torque. The ratio of the ultimate torque to the cracking torque depends mainly on the relative width of flanges. (Ersoy et al.,2003).

Beams having only longitudinal bars and beams having only hoops (or stirrups) behave similar to plain concrete beams. It seems that the presence of either longitudinal or transverse bars do not change the behavior significantly. However if these two type of reinforcement, i.e longitudinal bars and transverse reinforcement (spirals, stirrups or hoops) are used together, then the behavior changes significantly. After the initial cracking the reinforcement starts to be effective and the beam can carry torques much higher than the cracking torque. Instead of the single diagonal cracks observed in plain specimens, many cracks are formed as shown in Figure 3.10.(Ersoy et al.,2003).

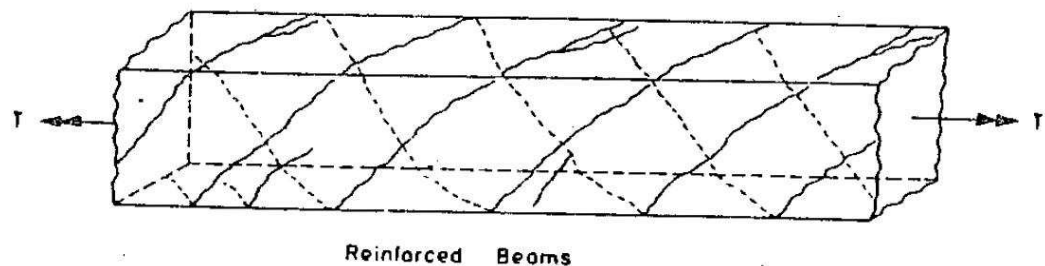


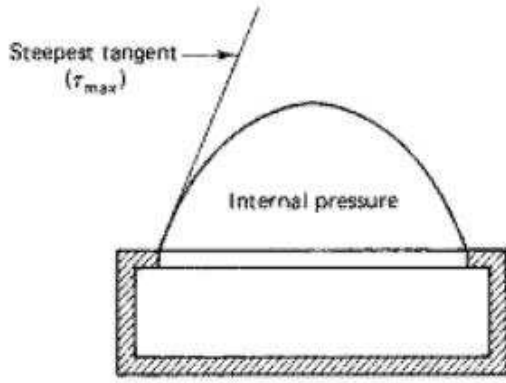
Figure 3.10 Reinforced Beams (Ersoy et al.,2003)

For over sixty years, the torsional analysis of concrete members has been based on either (1) the classical theory of elasticity developed through mathematical formulations coupled with membrane analogy verifications (St. Venant's) or (2) the theory of plasticity represented by the sand-heap analogy (Nadai's). Both theories were applied essentially to the state of pure torsion. But experiments revealed that the elastic theory is not entirely satisfactory for the accurate prediction of the state of stress in concrete in pure torsion. The behavior of concrete was found to be better represented by the plastic approach. Consequently, almost all developments in torsion as applied to concrete and reinforced concrete have been in the latter direction (Nawy,2005).

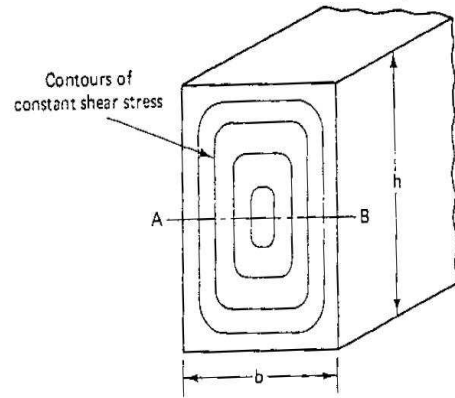
3.1.4 Torsion in Elastic Materials

In classical mechanics, torsional stresses can be computed by idealizing the properties of the material used. In the past, stresses in reinforced concrete members were calculated using the theory of elasticity. It was assumed that reinforced concrete is a homogeneous and linearly elastic material. The stress distribution obtained for rectangular sections using theory of elasticity. The stress distribution gets very complicated for flanged sections. In practice, theory of elasticity equations were simplified for such sections by dividing the cross-section into rectangles.(Ersoy et al.,2003)

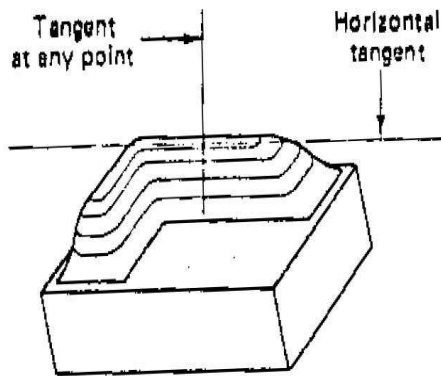
St. Venant presented in 1853 his solution to the elastic torsional problem with warping due to pure torsion that develops in noncircular sections. Prandtl in 1903 demonstrated the physical significance of the mathematical formulations by his membrane analogy model. The model establishes particular relationships between the deflected surface of the loaded membrane and the distribution of torsional stresses in a bar subjected to twisting moments. Figure 3.11 shows the membrane analogy behavior for rectangular as well as L-shaped forms. For small deformations, it can be proved that the differential equation of the deflected membrane surface has the same form as the equation that determines the stress distribution over the cross-section of the bar subjected to twisting moments. Similarly, it can be demonstrated that (1) the tangent to a contour line at any point of a deflected membrane gives the direction of the shearing stress at the corresponding cross-section of the actual member subjected to twist; (2) the maximum slope of the membrane at any point is proportional to the magnitude of shear stress at the corresponding point in the actual member; (3) the twisting moment to which the actual member is subjected is proportional to twice the volume under the deflected membrane. It can be seen from Figure 3.11 that the torsional shearing stress is inversely proportional to the distance between the contour lines. The closer the lines are, the higher the stress, leading to the previously stated conclusion that the maximum torsional shearing stress occurs: it the middle of the longer side of the rectangle. From the membrane analogy, this maximum stress has to be proportional to the steepest slope of the tangents at points *A* and *B* (Zhang,2002).



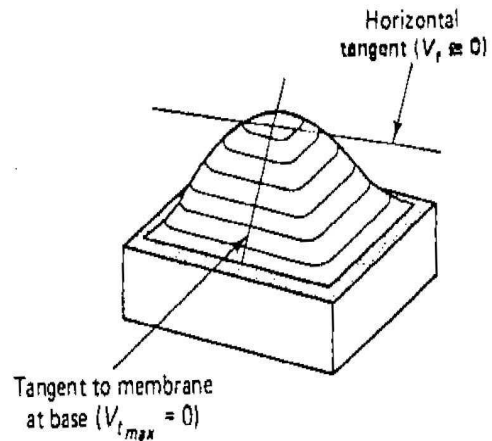
(a) membrane under pressure



(b) contours in a real beam or in a membrane



(c) L-section



(d) rectangular section

Figure 3.11 Membrane analogy in elastic pure torsion (Nawy,2005).

If δ = maximum displacement of the membrane from the tangent at point A, then from basic principles of mechanics and St. Venant's theory, (Nawy,2005).

$$\delta = b^2 G \theta \quad (3.9)$$

where G is the shear modulus and θ is the angle of twist. But $V_{t(\max)}$ is proportional to the slope of tangent; hence (Nawy,2005).

$$V_{t(\max)} = k_1 b G \theta \quad (3.10)$$

where the k 's are constants. The corresponding torsional moment T_ℓ is proportional to twice the volume under the membrane (Nawy,2005), or

$$T_\ell \propto 2 \left(\frac{2}{3} \delta b h \right) = k_2 \delta b h \quad (3.11)$$

or;

$$T_\ell = k_3 b^3 h G \theta \quad (3.12)$$

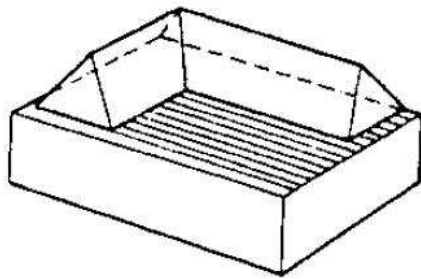
3.1.5 Torsion in Plastic Materials

As indicated earlier, the plastic sand-heap analogy provides a better representation of the behavior of brittle elements such as concrete beams subjected to pure torsion. The torsional moment is also proportional to twice the volume under the heap, and the maximum torsional shearing stress is proportional to the slope of the sand heap. Figure 3.12 is a two- and three-dimensional illustration of the sand heap. The torsional moment T_p in Figure 3.12 d is proportional to twice the volume of the rectangular heap shown in parts (b) and (c). It can also be recognized that the slope of the sand-heap sides as a measure of the torsional shearing stress is constant in the sand-heap analogy approach, whereas it is continuously variable in the membrane analogy approach. This characteristic of the sand heap considerably simplifies the solutions (Zhang,2002).

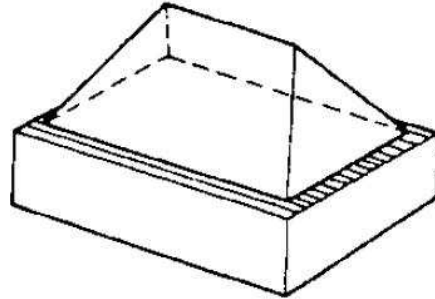
3.1.6 Sand-heap Analogy Applied to L Beams

Most concrete elements subjected to torsion are flanged sections, most commonly L beams comprising the external wall beams of a structural floor. The L beam in Figure 3.12 is chosen in applying the plastic sand-heap approach to evaluate

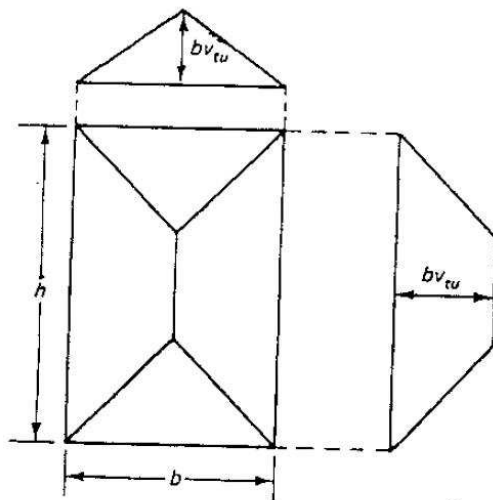
its torsional moment capacity and shear stresses to which it is subjected (Nawy,2005).



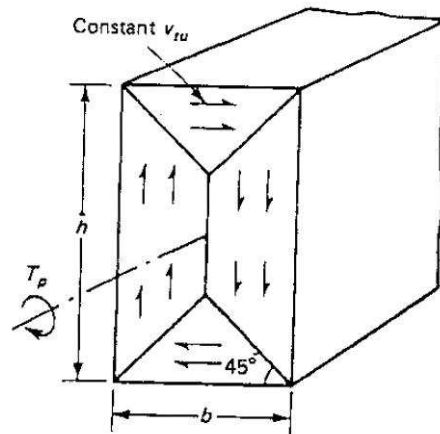
(a) sand-heap L-section



(b) sand-heap rectangular section



(b) plan of rectangular section



(d) torsional shear stress

Figure 3.12 Sand-heap analogy in plastic pure torsion (Nawy,2005)

The sand heap is broken into three volumes:

$$V_1 = \text{pyramid representing a square cross-sectional shape} = y_1 b_w^2 / 3$$

$$V_2 = \text{tent portion of the web representing a rectangular cross-sectional shape} = y_1 b_w (h - b_w) / 2$$

$$V_3 = \text{tent representing the flange of the beam, transferring part PDI to NQM} = y_2 h_f (b - b_w) / 2$$

Torsional moment is proportional to twice the volume of the sand heaps; hence

$$T_p = 2 \left[\frac{y_1 b_w^2}{3} + \frac{y_1 b_w (h - b_w)}{2} + \frac{y_2 h_f (b - b_w) / 2}{2} \right] \quad (3.13)$$

Also, torsional shear stress is proportional to the slope of the sand heaps; hence

$$y_1 = \frac{v_t b_w}{2} \quad (3.13a)$$

$$y_2 = \frac{v_t h_f}{2} \quad (3.13b)$$

Substituting y_1 and y_2 from Eqn. 3.13a and 3.13b into Eqn.3.13 gives us

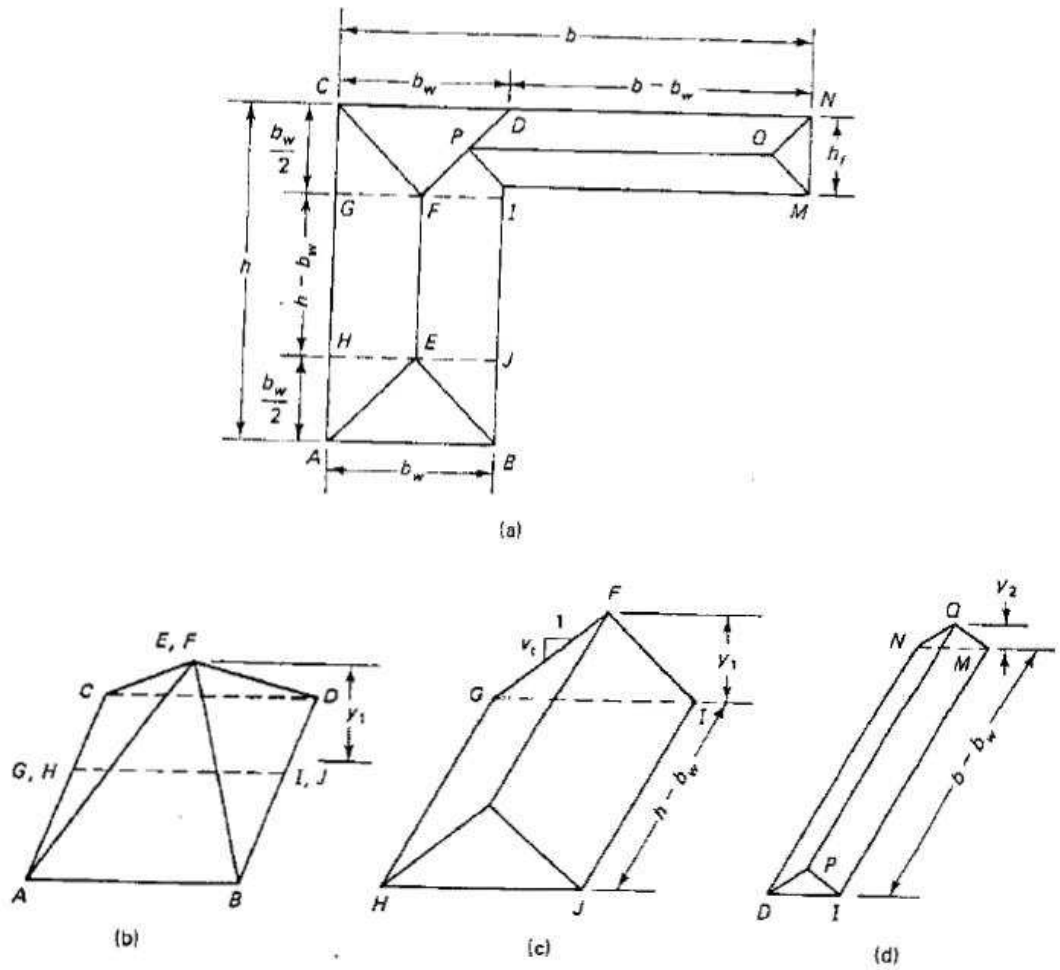


Figure 3.13 Sand-heap analogy of flanged section:

- (a) sand heap on L-shaped cross section;
- (b) composite pyramid from web V_1 ;
- (c) tent segment from web V_2 ;
- (d) transformed tent of beam flange V_3 (Nawy,2005).

$$V_{t(\max)} = \frac{T_p}{(b_w^2 / 6)(3h - b_w) + (h_f^2 / 2)(b - b_w)} \quad (3.14)$$

If both the numerator and denominator of Eqn.3.14 are divided by $(b_w h)^2$ and the terms rearranged, we have ;

$$V_{t(\max)} = \frac{T_p h / (b_w h)^2}{\left[\frac{1}{6} (3 - b_w / h) \right] + \left[\frac{1}{2} (h_f / b_w) 2(b / h - b_w / h) \right]} \quad (3.15a)$$

If one assumes that C_1 is the denominator in Eqn.3.15(a) and $J_E = C_1 (b_w h)^2$ Eqn.3.15(a) becomes

$$V_{t(\max)} = \frac{T_p h}{J_E} \quad (3.15b)$$

where J_E is the equivalent polar moment of inertia and a function of the shape of the beam cross section. Note that Eqn.3.15(b) is similar in format to from the membrane analogy except for the different values of the denominator J and J_E . Eqn 3.15(a) can be readily applied to rectangular section by setting $h=0$ (Nawy,2005).

It must also be recognized that concrete is not a perfectly plastic material; hence the actual torsional strength of the plain concrete section has a value lying between the membrane analogy and the sand-hcap analogy values. Eqn 3.15(b) can be rewritten designating $T_p = T_c$ as the nominal torsional resistance of the plain concrete and $V_{t(\max)} = V_{tc}$ using ACI terminology, so that

$$T_c = k_2 b^2 h V_{tc} \quad (3.16a)$$

$$T_c = k_2 x^2 y V_{tc} \quad (3.16b)$$

where x is the smaller dimension of the rectangular section (Nawy,2005).

Extensive work by Hsu, confirmed by others, has established that k_2 , can be taken as $\frac{1}{3}$. This value originated from research in the skew-bending theory of plain concrete. It was also established that $6\sqrt{f'_c}$ can be considered as a limiting value of the pure torsional strength of a member without torsional reinforcement (Nawy,2005).

Using a reduction factor of 2.5 for the first cracking torsional load $V_{tc} = 2.4\sqrt{f'_c}$ and using $k_2 = \frac{1}{3}$ in Eqn.3.16 results in

$$T_c = 0.8\sqrt{f'_c}x^2y \quad (3.17a)$$

where x is the shorter side of the rectangular section. The high reduction factor of 2.5 is used to offset any effect of shear and bending moments that might be present.

If the cross section is a T or L section, the area can be broken into component rectangles as in Figure 3.14, (Nawy,2005) such that

$$T_c = 0.8\sqrt{f'_c} \sum x^2y \quad (3.17b)$$

3.1.7 Skew-Bending Theory

This theory considers in detail the internal deformation behavior of a series of transverse warped surfaces along the beam. Initially presented by Lessig in 1958, it had subsequent contributions from several researchers in this field (Nawy,1985). Studies by Hsu have led to the conclusion that failure of a rectangular section in

torsion occurs by bending about an axis parallel to the wider face of the section, and inclined at about 45° to the longitudinal axis of the beam (Hsu,1984).

In previous versions of ACI code (from 1971 to 1989) (ACI,1971 and ACI,1989), torsional strength of beams was calculated by using this theory. According to the codes, torsional strength T_n of beams was considered to be made up of two parts: one part is contributed by concrete T_c while the other part is contributed by web reinforcement T_s . Hsu on hollow and solid rectangular beams, it was observed that the concrete core does not contribute to the ultimate torsional strength (Hsu,1968). Later he concluded that the concrete contribution T_c was mainly due to the shear resistance of the diagonal concrete struts (Çevik et al.,2009).

The post-cracking behaviour of reinforced concrete members may be alternatively studied on the basis of the mechanism of failure rather than on the basis of stresses. In the consideration of the failure mechanism, the combined action of torsion with flexure and shear has to be taken into account. (Nawy,2005).

The failure surface of the normal beam cross section subjected to bending moment M_u remains plane after bending, as in Figure 3.14(a). If a twisting moment T_u is also applied exceeding the capacity of the section, cracks develop on three sides of the beam cross-section and compressive stresses on portions of the fourth side along the beam. As torsional loading proceeds to the limit state at failure, a skewed failure surface results due to the combined torsional moment T_u and bending moment M_u . The neutral axis of the skewed surface and the shaded area in Figure 3.14(b) denoting the compression zone would no longer be straight but subtend a varying angle θ with the original plane cross-sections (Nawy,2005).

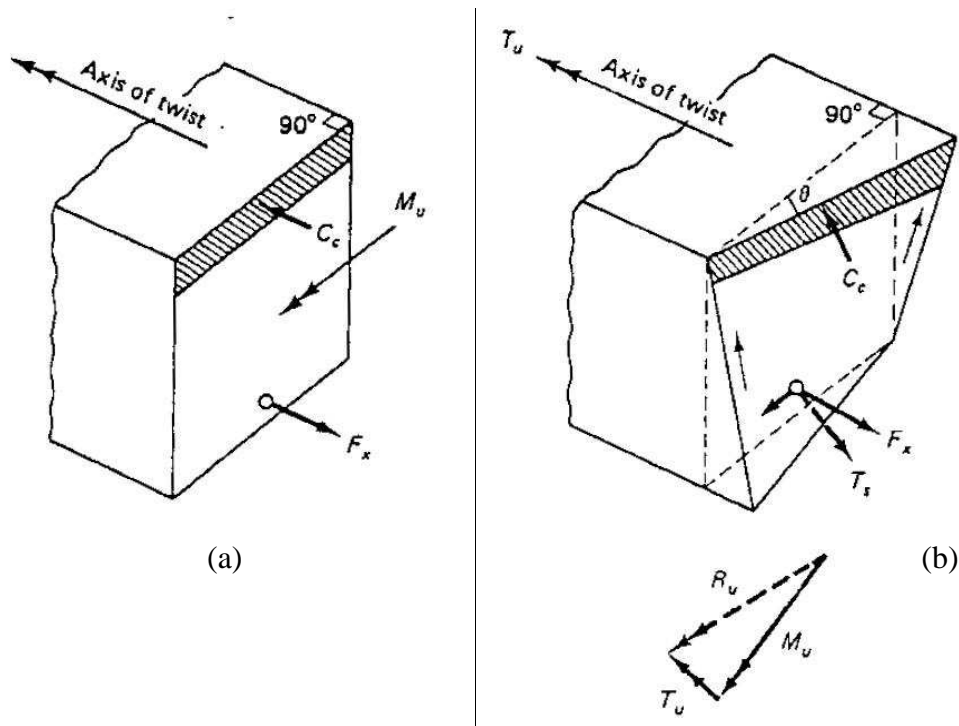
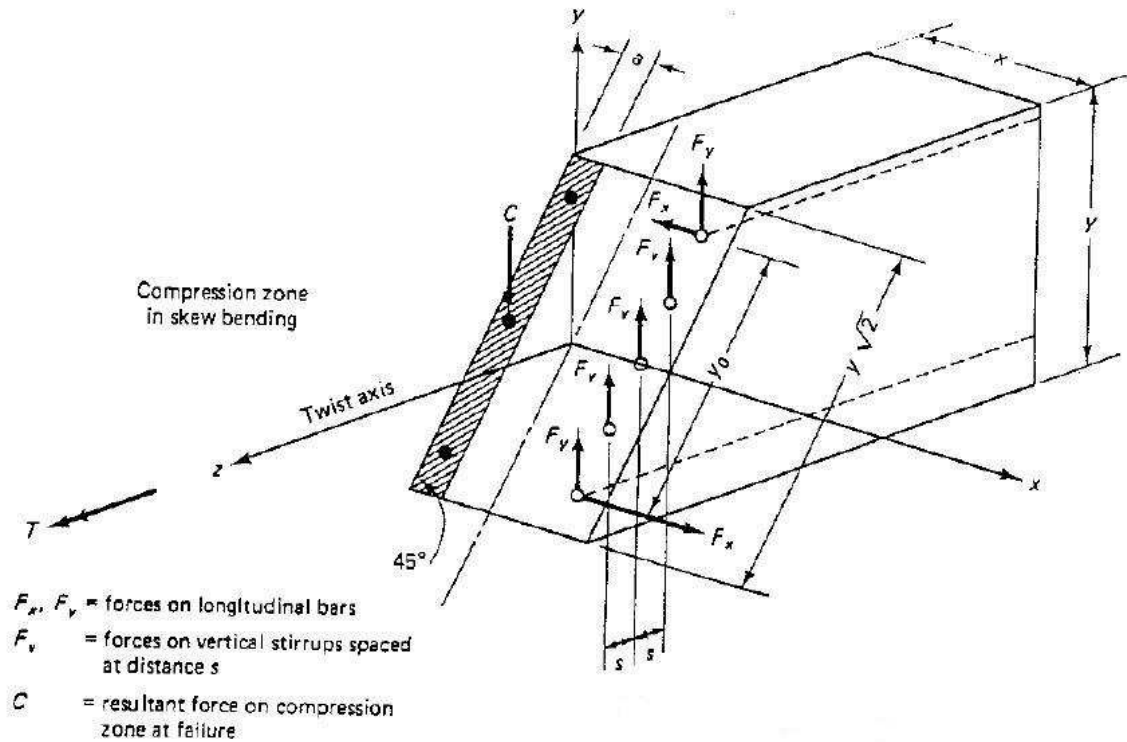


Figure 3.14 Skew bending due to torsion: (a) bending before twist; (b) bending and torsion (Nawy,2005).

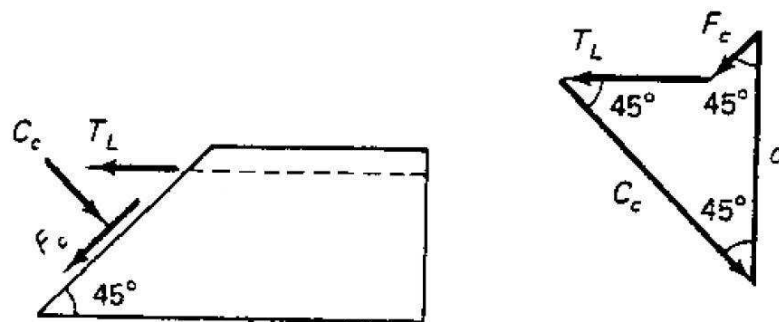
Prior to cracking, neither the longitudinal bars nor the closed stirrups make any appreciable contribution to the torsional stiffness of the section. At the post-cracking stage of loading, the stiffness of the section is reduced, but its torsional resistance is considerably increased, depending on the amount and distribution of both the longitudinal bars and the transverse closed ties. It has to be emphasized that little additional torsional strength can be achieved beyond the capacity of the plain concrete in the beam unless both longitudinal torsion bars and transverse ties are used. (Nawy,2005).

The skew-bending theory idealizes the compression zone by considering it to be of uniform depth. It assumes the cracks on the remaining three faces of the cross section to be uniformly spread, with the steel ties (stirrups) at those faces carrying the tensile forces all the cracks and the longitudinal bars resisting shear through dowel action with the concrete Figure 3.15(a) shows the forces acting on the skewlv bent plane (Nawy,2005).

The polygon in Figure 3.15(b) gives the shear resistance F_c of the concrete, the force T_t of the active longitudinal steel bars in the compression zone, and the normal compressive block force C_u .



(a)



(b)

Figure 3.15. Forces on the skewly bent planes: (a) all forces acting on skew plane at failure; (b) vector forces on compression zone Nilson and Winter,(1991).

The torsional moment T_c of the resisting shearing force F_c generated by the shaded compressive block area in Figure 3.15 a is thus

$$T_c = \frac{F_c}{\cos 45^\circ} \times (\text{its arm about forces } F_v) \quad \text{in Fig 3.15 a}$$

or

$$T_c = \sqrt{2}F_c(0.8x) \quad (3.18a)$$

where x is the shorter side of the beam. Extensive tests to evaluate F_c in terms of internal stress in concrete $k_1\sqrt{f'_c}$ and the geometrical torsional constants of the section k_2x^2y led to the expression (Nawy,2005).

$$T_c = \frac{2.4}{\sqrt{x}} x^2 y \sqrt{f'_c} \quad (3.18b)$$

3.1.8 Torsion in Reinforced Concrete Elements

Torsion rarely occurs in concrete structures without being accompanied by bending and shear. The foregoing should give a sufficient background on the contribution of the plain concrete in the section toward resisting part of the combined stresses resulting from torsional, axial, shear, or flexural forces. The capacity of the plain concrete to resist torsion when in combination with other loads could, in many cases, be lower than when it resists the same isolated external twisting moments alone. Consequently, torsional reinforcement has to be provided to resist the excess torque (Nawy,2005).

Inclusion of longitudinal and transverse reinforcement to resist part of the torsional moments introduces a new element in the set of forces and moments in the section.

T_n = required total nominal torsional resistance of the section including the reinforcement

T_c = nominal torsional resistance of the plain concrete

T_x = torsional resistance of the reinforcement

Then;

$$T_n = T_c + T_x \quad (3.19)$$

T_c is assumed equal to zero for design simplification, and all the torsion is assumed to be borne by the longitudinal steel bars and the closed transverse stirrups. To study the contribution of the longitudinal steel bars and the closed stirrups, one has to analyze the system of forces acting on the warped cross-sections of the structural element at the limit state of failure. A modified space truss analogy is presented comparable to the plane truss analogy used for the design of shear stirrups. In this theory, both the longitudinal reinforcement and the transverse stirrups (ties) are utilized as components of the space truss (Nawy,2000).

3.1.9 Space Truss Analogy Theory

Torsional capacity of a concrete member reinforced both longitudinally and transversely can be obtained by forming a space truss model. Truss analogy for torsion was first developed by Rausch in 1929. Similar to the assumption made in the truss model for shear, it was assumed that after cracking concrete can not carry any tension. In the analogous space truss, concrete compressive struts between the diagonal cracks were taken as diagonals, longitudinal steel as tension chords and transverse steel bars were taken as tension members. The space truss model used is illustrated in Figure 3.15. (Ersoy et al.,2003)

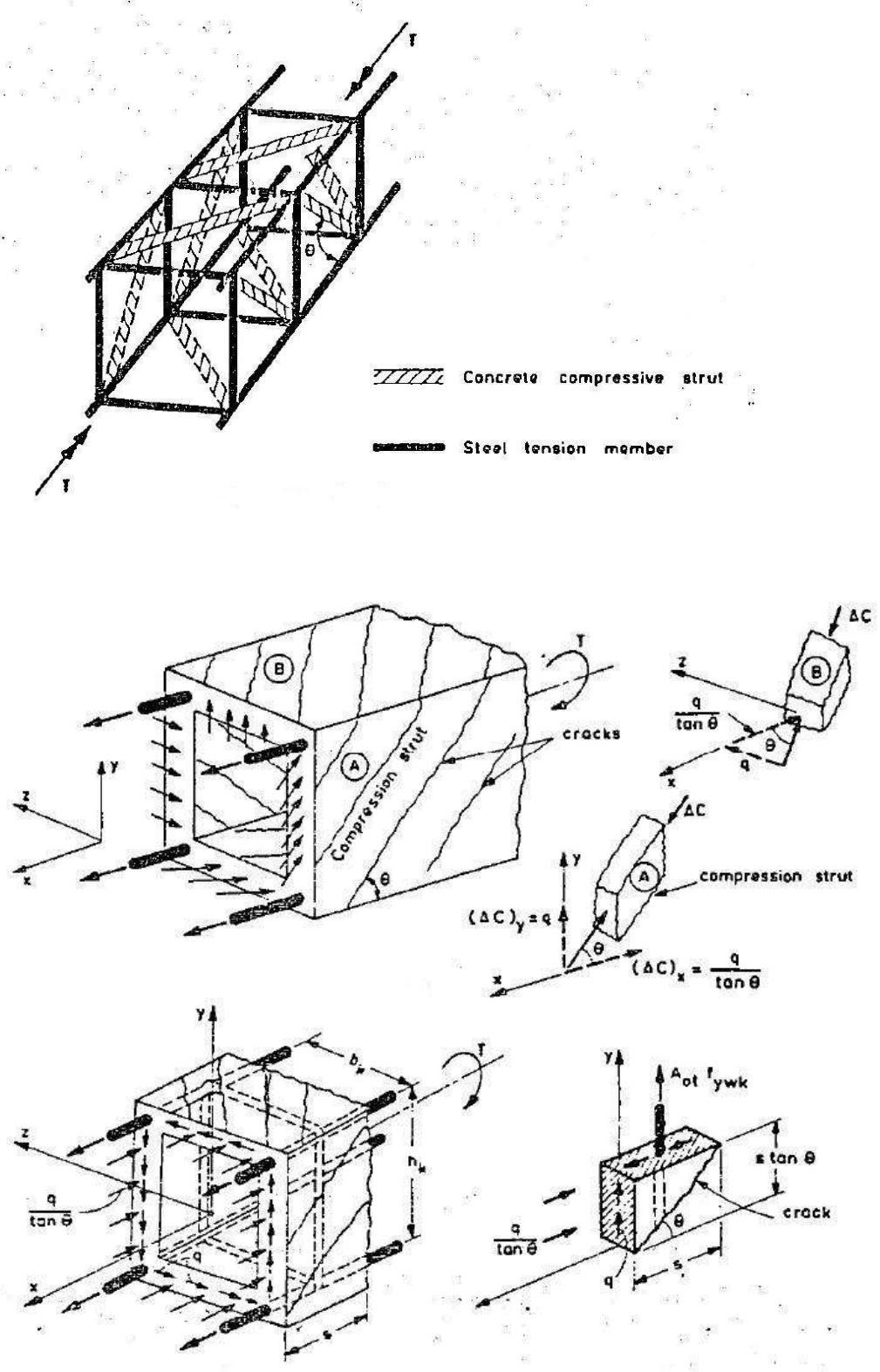


Figure 3.16 Space Truss Model (Ersoy et al.,2003).

In Figure 3.16 section cut perpendicular to the axis (x-axis) of the member is shown. For illustrative reasons the concrete is shown as a tubular section rather than a solid section. This doesn't create any serious error, since as would be recalled from elementary theories on torsion, internal fibers are not very effective in resisting the torque. (Nawy,2005).

The section shown cuts the concrete compressive struts all around the periphery. The compressive forces acting on the struts cut by the section taken are marked on the figure. The inclined compressive forces acting along the periphery have to be resisted mainly by the transverse and longitudinal reinforcement. (Nawy,2005).

In Figure 3.16 struts A and B, included between two diagonal cracks, are taken as free bodies. It is assumed that there is no transfer of stresses at the crack face. The only force on the strut is AC which is the uniaxial force per unit length of the perimeter. (Nawy,2005).

It is assumed in this theory that the concrete beam behaves in torsion similar to a thin-walled box with a constant shear flow in the wall cross-section, producing a constant torsional moment. The use of hollow-walled sections rather than solid sections proved to give essentially the same ultimate torsional moment, provided that the walls are not too thin. Such a conclusion is borne out by tests, which have shown that the torsional strength of the solid sections is composed of the resistance of the closed stirrup cage, consisting of the longitudinal bars and transverse stirrups, and the idealized concrete inclined compression struts in the plane of the cage wall. The compression struts are the inclined concrete strips between the cracks in Figure 3.17. (Hassoun,1985).

The CFB-FIP code is based on the space truss model. In this code, the effective wall thickness of the hollow beam is taken as $\frac{1}{6}D_a$ where D_a is the diameter of the circle inscribed in the rectangle connecting the corner longitudinal bars; that is $D_a = x_a$ in Figure 3.17. (Nawy,2005).

A rational method to derive the effective wall thickness was given by Hsu (Nawy,2000). This nonlinear analysis takes into account the warping compatibility condition of the wall. In summary, the absence of the core does not affect the strength of such members in torsion: hence the acceptability of the space truss analogy approach based on hollow box. (Nawy,2005)

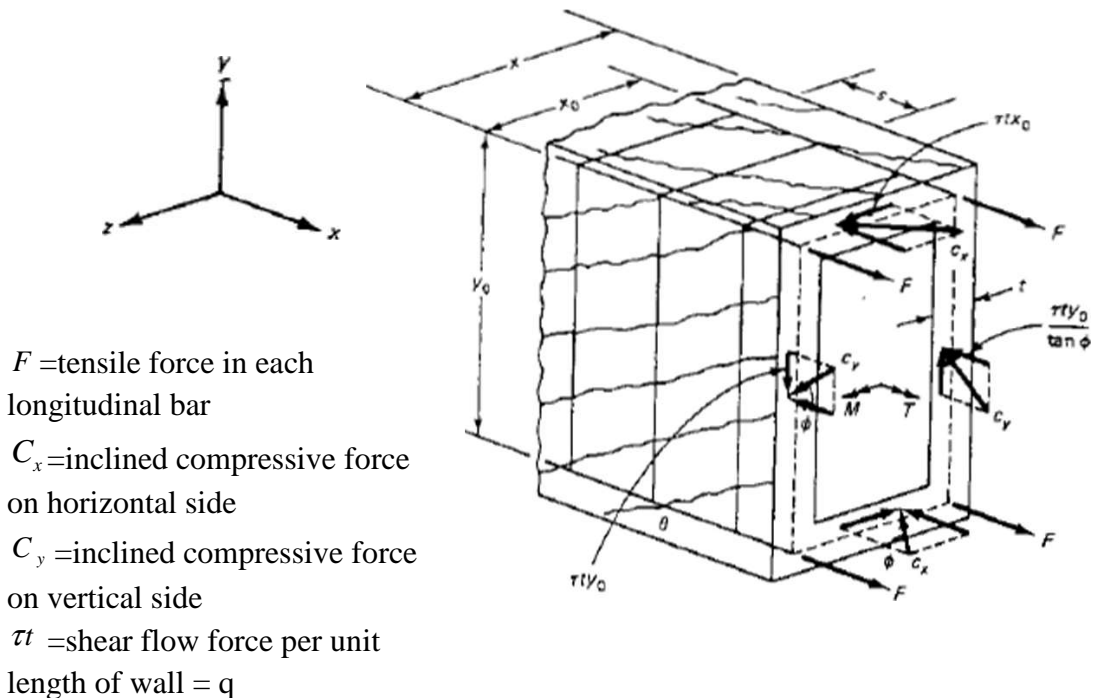


Figure 3.17 Forces on hollow box concrete surface by truss analogy (Nawy,2005).

3.1.10 Equilibrium in Element Shear

A unit square membrane element of thickness h is subjected to shear flow q due to pure shear as in Figure 3.18 (Nawy,2000). Reinforcement in both the longitudinal (E-W) direction ℓ and transverse (N-S) direction t is subjected to a unit stress f_ℓ / s_ℓ and f_t / s_t respectively such that the shear flow q can be defined by the equilibrium equations

$$q = F_\ell \tan \theta \quad (3.20a)$$

where unit $F_\ell = A_\ell f_\ell / s_t$ and ;

$$q = F_t \cot \theta \quad (3.20b)$$

where unit $F_t = A_t f_t / s$, A is the cross-sectional area of the reinforcement, s_t and s are the spacings in the t and ℓ directions, respectively.

From the geometry of the triangles in Figure 3.18, the shear flow can also be defined as;

$$q = (f_D t) \sin \theta \cos \theta \quad (3.20c)$$

If the reinforcement in both directions is assumed to have yielded. Eqn.3.20(a) and (b) give

$$\tan \theta = \sqrt{\frac{F_{ty}}{F_{\ell y}}} \quad (3.21a)$$

and
$$q_y = \sqrt{F_{\ell y} F_{ty}} \quad (3.21b)$$

where the subscript y denotes the yielding of reinforcement.

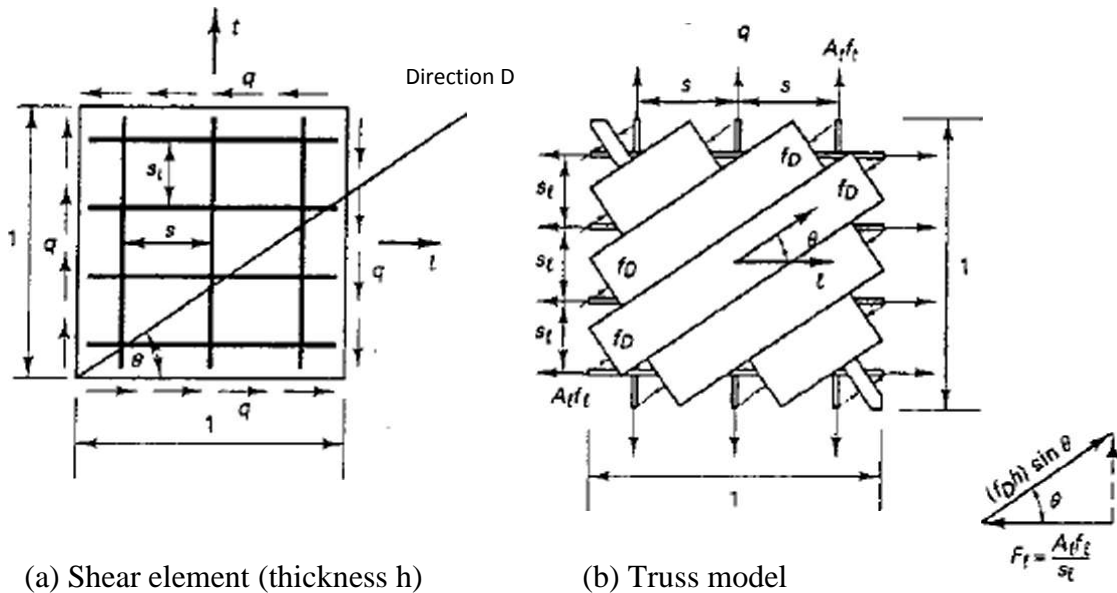


Figure 3.18 Equilibrium forces in element shear (Nawy,2000).

3.1.11 Equilibrium in Element Torsion

The case of a hollow tube of any shape and variable thickness is considered Figure 3.19. It is subjected to pure torsion. St. Venant's theory stipulates that the cross-sectional shape remains unchanged in elastic small deformations, and the warping deformation perpendicular to the cross-section would be the same along the member's axis. Hence it can be assumed that only shear stresses develop in the tube wall in the form of shear flow q in Figure 3.19(a) and that the in-plane normal stresses in the wall vanish (Nawy,2005). If an infinitesimal wall element ABCD is isolated as in Figure 3.19(b) the shear flow in the ℓ direction has to be equal to the shear flow in the t direction or

$$\tau_1 t_1 = \tau_2 t_2 \quad (3.22)$$

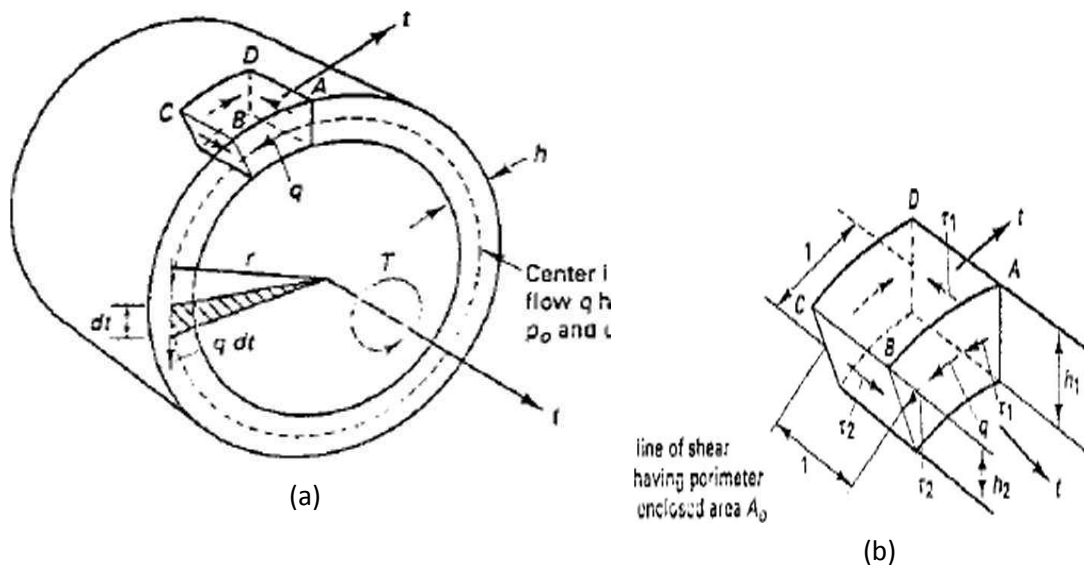


Figure 3.19 Hollow tube equilibrium torsion forces:

(a) section of tube subjected to torsion T ; (b) unit shear element from tube wall of varying thickness h , Note: ℓ and t denote the longitudinal and transverse directions, respectively (Nawy,2005).

3.1.12 Shear-Torsion-Bending Interaction

Consider the rectangular boxes in Figures 3.19. The shear flow q will not be the same on the four walls of the box when subjected to combined shear and torsion. Failure can precipitate in two distinct modes:

- (a) Yielding of the longitudinal bottom tension steel and the transverse stirrups
- (b) Yielding of the longitudinal top compression steel and the transverse stirrups

(a) Bottom tension steel yielding. If the failure mode is caused by yielding of the longitudinal bottom stringer (tensile steel) and the transverse stirrups due to combined shear and torsion, the following expression can be derived from equilibrium (Nawy,2000).

$$\frac{M}{F_B y_0} + \left(\frac{V}{2y_0} \right)^2 \frac{y_0}{F_B} \frac{s}{A f_{yt}} + \left(\frac{T}{2A_0} \right)^2 \frac{y_0 + x_0}{F_B} \frac{s}{A f_{yt}} = 1 \quad (3.23)$$

If M_0 , V_0 and T_0 are the moments and forces acting alone they can be defined as follows:

$$M_0 = F_B y_0 \quad (3.24a)$$

$$V_0 = 2y_0 \sqrt{\frac{F_T A f_v}{y_0 s}} \quad (3.24b)$$

for a two web box.

$$T_0 = 2A_0 \sqrt{\frac{2F_T A f_v}{p_0 s}} \quad (3.24c)$$

where $p_0 = 2(y_0 + x_0)$

$$R = \frac{F_T}{F_B} \quad (3.24d)$$

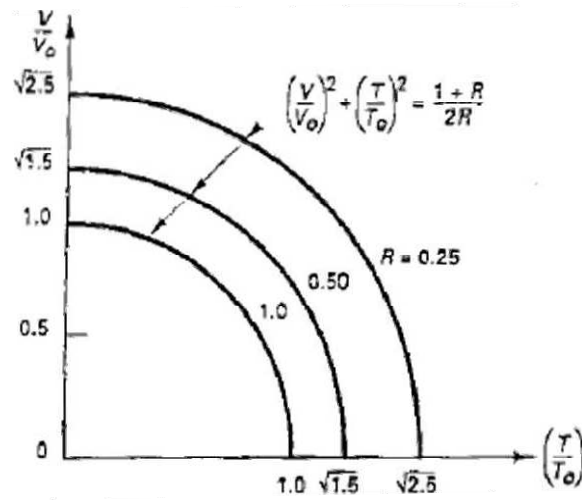


Figure 3.20 Shear-torsion interaction diagram (Nawy,2005).

A nondimensional interaction surface relationship can be obtained by introducing Eqn 3.24 into Eqn 3.23 such that

$$\left(\frac{M}{M_0}\right) + \left(\frac{V}{V_0}\right)^2 R + \left(\frac{T}{T_0}\right)^2 R = 1 \quad (3.25a)$$

(b) Top compression steel yielding. If the failure mode is caused by yielding of the longitudinal top chord (compression steel) and the transverse stirrups, Eqn. 3.25(a) becomes

$$-\left(\frac{M}{M_0}\right)\frac{1}{R} + \left(\frac{V}{V_0}\right)^2 + \left(\frac{T}{T_0}\right)^2 = 1 \quad (3.25b)$$

From both Eqn 3.25(a) and (b) the interaction of V and T is circular for a constant bending moment M for both failure surfaces. The intersection of the two

failure surfaces for these two failure modes forms a peak interaction curve between V and T such that Eqn 3.25(a) and (b) give

$$\left(\frac{V}{V_0}\right)^2 + \left(\frac{T}{T_0}\right)^2 = \frac{1+R}{2R} \quad (3.26a)$$

Equation 3.26(a) for $R = 0.25, 0.5$ and 1.0 on the peak planes gives the circular plots shown in Figure 3.20. A third mode of failure is caused by yielding in the top bar, in the bottom bar, and in the transverse reinforcement, all on the side where shear flows due to shear and torsion are additive, that is the left wall (Nawy,2000). A modified form of Eqn 3.26(a) results as follows:

$$\left(\frac{V}{V_0}\right)^2 + \left(\frac{T}{T_0}\right)^2 + \sqrt{2}\left(\frac{VT}{V_0T_0}\right) = \frac{1+R}{2R} \quad (3.26b)$$

3.2 Aci Design Of Reinforced Concrete Beams Subjected To Combined Torsion Bending And Shear

3.2.1 Torsional Behavior of Structures

The torsional moment acting on a particular structural component such as a spandrel beam can be calculated using normal structural analysis procedures. Design of the particular component needs to be based on the limit state at failure. Therefore, the nonlinear behavior of a structural system after torsional cracking must be identified in one of the following two conditions: (1) no redistribution of torsional stresses to other members after cracking and (2) redistribution of torsional stresses and moments after cracking to effect deformation compatibility between intersecting members (Nawy,2005).

Stress resultants due to torsion in statically determinate beams can be evaluated from equilibrium conditions alone. Such conditions require a design for the full-factored external torsional moment, because no redistribution of torsional stresses

is possible. This state is often termed equilibrium torsion. An edge beam supporting a cantilever canopy (Nawy, 2005).

The edge beam has to be designed to resist the total external factored twisting moment due to the cantilever slab; otherwise, the structure will collapse. Failure would be caused by the beam not satisfying conditions of equilibrium of forces and moments resulting from the large external torque (Nawy, 2005).

In statically indeterminate systems, stiffness assumptions, compatibility of strains at the joints, and redistribution of stresses may affect the stress resultants, leading to a reduction in the resulting torsional shearing stresses. A reduction is permitted in the value of the factored moment used in the design of the member if part of this moment can be redistributed to the intersecting members. The ACI Code permits a maximum factored torsional moment at the critical section d from the face of the supports for reinforced concrete members as follows (Nawy, 2005) :

$$T_a = \phi 4 \sqrt{f'_c} \frac{A_{cp}^2}{p_{cp}} \quad (3.27)$$

where

A_{cp} = area enclosed by outside perimeter of concrete cross section

$$= x_0 y_0$$

p_{cp} = outside perimeter of concrete cross section A_{cp} in.

$$= 2(x_0 + y_0)$$

3.2.2 Torsional Moment Strength

The size of a cross-section is chosen on the basis of reducing unsightly cracking and preventing the crushing of the surface concrete caused by the inclined compressive stresses due to shear and torsion defined by the left-hand side of the expressions in Eqn.3.28(a) and (b). The geometrical dimensions for torsional moment strength in both reinforced and prestressed members are limited by the following expressions (Nawy,2005).

(a) Solid sections

$$\sqrt{\left(\frac{V_u}{b_w d}\right)^2 + \left(\frac{T_u P_h}{1.7 A_{0h}^2}\right)^2} \leq \phi \left(\frac{V_c}{b_w d} + 8\sqrt{f'_c} \right) \quad (3.28a)$$

(b) Hollow section

$$\left(\frac{V_u}{b_w d} \right) + \left(\frac{T_u P_h}{1.7 A_{0h}^2} \right) \leq \phi \left(\frac{V_c}{b_w d} + 8\sqrt{f'_c} \right) \quad (3.28b)$$

CHAPTER 4

GENETIC PROGRAMMING

4.1 Genetic Programming Systems

4.1.1 Genetic Programming

Genetic algorithm (GA) is an optimization and search technique based on the principles of genetics and natural selection. A GA allows a population composed of many individuals to evolve under specified selection rules to a state that maximizes the “fitness” (i.e., minimizes the cost function). The method was developed by John Holland (Holland, J. H. ,1975) and finally popularized by one of his students, David Goldberg (Goldberg,D. E.,1989), solved a difficult problem involving the control of gas-pipeline transmission for his dissertation (Haupt RL and Haupt SE,2004). The fitness of each individual in a genetic algorithm is the measure the individual has been adapted to the problem that is solved employing this individual. It means that fitness is the measure of optimality of the solution offered, as represented by an individual from the genetic algorithm. The basis of genetic algorithms is the selection of individuals in accordance with their fitness; thus, fitness is obviously a critical criterion for optimization (Chambers,L.,2001).

Genetic Programming is an extension to Genetic Algorithms proposed by Koza (Koza,1992). The early pioneer defines GP as a domain-independent problem-solving approach in which computer programs are evolved to solve, or approximately solve, problems based on the Darwinian principle of reproduction and survival of the fittest and analogs of naturally occurring genetic operations such as crossover (sexual recombination) and mutation. GP reproduces computer programs to solve problems by executing the following steps which involves:

1) Generation of an initial population of functions and terminals of the problem (computer programs).

2) Execution of each program in the population and assigning fitness, respectively.

3) Repeating step 2 for new computer programs.

4) Selecting the best existing program which is presented as the result of genetic programming (Koza,1992).

In this study GEP (gene expression Programming) is used which is an extension to GP. Genetic programming is a domain-independent method that genetically breeds a population of computer programs to solve a problem. Specifically, genetic programming iteratively transforms a population of computer programs into a new generation of programs by applying analogs of naturally occurring genetic operations. The genetic operations include crossover (sexual recombination), mutation, reproduction, gene duplication and gene deletion. Analogous of developmental processes that transform an embryo into a fully developed entity are also employed. Genetic programming is an extension of the genetic algorithm. (Koza JR et al.,2003).

Gene expression programming belongs to a wider group of genetic algorithms as it uses populations of individuals, selects individuals according to fitness, and introduces genetic variation using one or more genetic operators.(Cevik,A.,2008)

The phenotype of GEP individuals consists of the same kind of diagram representations used by GP. However, these complex entities are encoded in simpler, linear structures of fixed length - the chromosomes. Thus, the main players in GEP are two entities: the chromosomes and the ramified structures or expression trees (ETs), being the latter the expression of the genetic information encoded in the former. The process of information decoding (from the chromosomes to the ETs) is

called translation. And this translation implies obviously a kind of code and a set of rules. The genetic code is very simple: a one-to-one relationship between the symbols of the chromosome and the functions or terminals they represent. The rules are also very simple: they determine the spatial organization of the functions and terminals in the ETs and the type of interaction between sub-ETs in multigenic systems (Ferreira C.,2001-Ireland JC,2002-Candida F.,2001).

In GEP there are therefore two languages: the language of the genes and the language of ETs and, in this simple replicator/phenotype system, knowing the sequence or structure of one, are knowing the other. In nature, although the inference of the sequence of proteins given the sequence of genes and vice versa is possible, practically nothing is known about the rules that determine the three-dimensional structure of proteins. But in GEP thanks to the simple rules that determine the structure of ETs and their interactions, it is possible to infer exactly the phenotype given the sequence of a gene, and vice versa. This bilingual and unequivocal system is called Karva language (Ferreira C.,2001-Ireland JC,2002-Candida F.,2001).

4.1.2 Solving a Simple Problem with GEP

For each problem, the type of linking function, as well as the number of genes and the length of each gene, are a priori chosen for each problem. While attempting to solve a problem, one can always start by using a single-gene chromosome and then proceed by increasing the length of the head. If it becomes very large, one can increase the number of genes and obviously choose a function to link the sub-ETs. One can start with addition for algebraic expressions or for Boolean expressions, but in some cases another linking function might be more appropriate (like multiplication or IF, for instance). The idea, of course, is to find a good solution, and GEP provides the means of finding one very efficiently.(www.gepsoft.com)

As an illustrative example consider the following case where the objective is to show how GEP can be used to model complex realities with high accuracy. So, suppose one is given a sampling of the numerical values from the curve (remember, however, that in real-world problems the function is obviously unknown)

:

$$y = 3a^2 + 2a + 1 \quad (4.1)$$

over 10 randomly chosen points in the real interval [-10, +10] and the aim is to find a function fitting those values within a certain error. In this case, a sample of data in the form of 10 pairs (a_i, y_i) is given where a_i is the value of the independent variable in the given interval and y_i is the respective value of the dependent variable (a_i values: -4.2605, -2.0437, -9.8317, -8.6491, 0.7328, -3.6101, 2.7429, -1.8999, -4.8852, 7.3998; the corresponding y_i values can be easily evaluated). These 10 pairs are the fitness cases (the input) that will be used as the adaptation environment. The fitness of a particular program will depend on how well it performs in this environment (Ferreira C.,2001)

There are five major steps in preparing to use gene expression programming. The first is to choose the fitness function. For this problem one could measure the fitness f_i of an individual program i by the following expression:

$$f_i = \sum_{j=1}^{C_t} (M - |C_{(i,j)} - T_j|) \quad (4.2)$$

where M is the range of selection, $C_{(i,j)}$ the value returned by the individual chromosome i for fitness case j (out of C_t fitness cases) and T_j is the target value for fitness case j . If, for all j , $|C_{(i,j)} - T_j|$ (the precision) less than or equal to 0.01, then the precision is equal to zero, and $f_i = f_{max} = C_t * M$. For this problem, use an $M = 100$ and, therefore, $f_{max} = 1000$. The advantage of this kind of fitness function is that the system can find the optimal solution for itself. However there are other fitness functions available which can be appropriate for different problem types (Ferreira C.,2001).

The second step is choosing the set of terminals T and the set of functions F to create the chromosomes. In this problem, the terminal set consists obviously of the independent variable, i.e., $T = \{a\}$. The choice of the appropriate function set is not so obvious, but a good guess can always be done in order to include all the necessary functions. In this case, to make things simple, use the four basic arithmetic operators.

Thus, $F = \{+, -, *, /\}$. It should be noted that there many other functions that can be used.

The third step is to choose the chromosomal architecture, i.e., the length of the head and the number of genes.

The fourth major step in preparing to use gene expression programming is to choose the linking function. In this case we will link the sub-ETs by addition. Other linking functions are also available such as subtraction, multiplication and division.

And finally, the fifth step is to choose the set of genetic operators that cause variation and their rates. In this case one can use a combination of all genetic operators (mutation at $p_m = 0.051$; IS and RIS transposition at rates of 0.1 and three transposons of length 1, 2, and 3; one-point and two-point recombination at rates of 0.3; gene transposition and gene recombination both at rates of 0.1). To solve this problem, lets choose an evolutionary time of 50 generations and a small population of 20 individuals in order to simplify the analysis of the evolutionary process and not fill this text with pages of encoded individuals. However, one of the advantages of GEP is that it is capable of solving relatively complex problems using small population sizes and, thanks to the compact Karva notation; it is possible to fully analyze the evolutionary history of a run. A perfect solution can be found in generation 3 which has the maximum value 1000 of fitness. The sub-ETs codified by each gene are given in Figure 1. Note that it corresponds exactly to the same test fuction given above in Eqn 4.1 (Ferreira C.,2001).

Thus expressions for each corresponding Sub-ET can be given as follows:

$$y = (a^2 + a) + (a + 1) + (2a^2) = 3a^2 + 2a + 1 \quad (4.3)$$

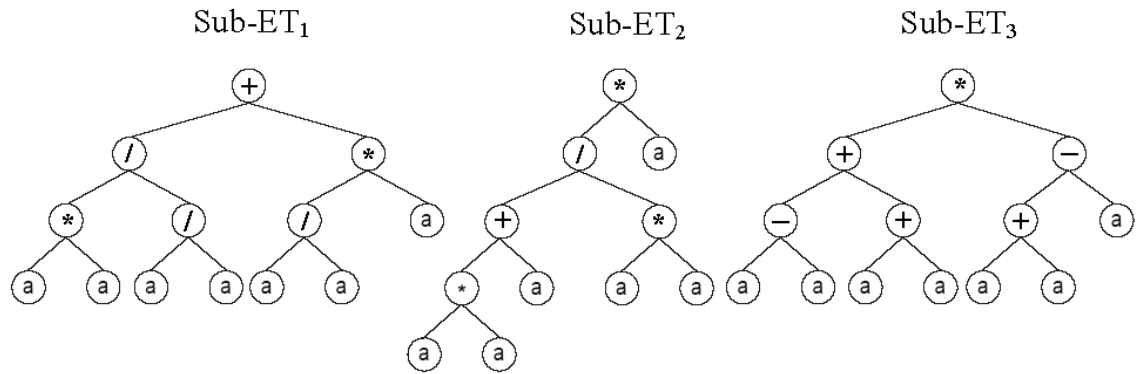


Figure 4.1. ET for the problem of Equation 4.1 (Ferreira C.,2001).

The whole flowchart of GEP process in general can be seen in Figure 4.2.

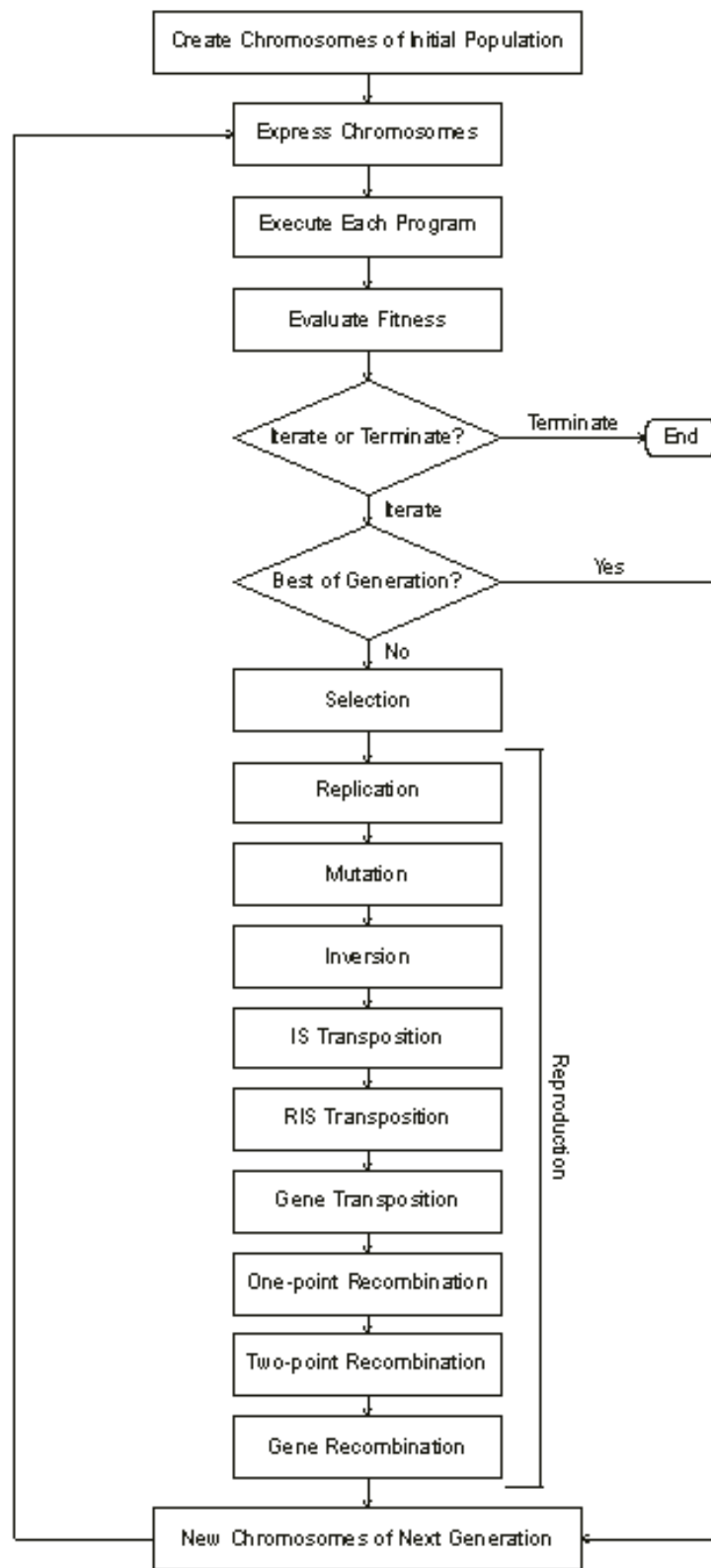


Figure 4.2 Gene Expression Programming Flowchart (www.gepsoft.com)

CHAPTER 5

NUMERICAL APPLICATION

5.1 Numerical application

In this study, GeneXproTools 4.0 (www.gepsoft.com) software package is used for GP modeling of torsional strength of RC beams. Among the experimental database, 17 tests were used as testing set and the remaining 59 test as training set for GP training. The proposed GP formula is an empirical equation based on the experimental database given here. In the proposed GP model, input parameters were selected based on previously published studies by Fang and Shiau (2004), Hsu (1968), Koutchoukali and Belarbi (2001) and Rasmussen and Baker (1995) which are area ($A_c = x.y$), perimeter ($P_c = 2(x+y)$), concrete compressive strength (f_c), total area of longitudinal torsional reinforcement \times yield strength of longitudinal torsional reinforcement ($A_l f_{yl}$), cross-sectional area of one leg of closed stirrup \times yield strength of torsional reinforcement/ spacing of stirrups, ($A_t f_{yt}/s$), steel ratio of stirrups (ρ_t) and steel ratio of longitudinal reinforcement (ρ_l). the ranges of variables in the experimental database where the proposed GP model will be valid for are given in Table 5.1. (Cevik et al.,2010)

The experimental database considered here (Table A.1) was collected from various studies Rasmussen and Baker (1995), Koutchoukali and Belarbi (2001), Fang and Shiau (2004), Hsu(1968), Tang(2006), Zang(2002). Test specimens of the database were of solid rectangular beams subjected to pure tension and where none of them was deep beam. The compressive strength of concrete ranged from 25.58 MPa to 109.8 MPa, stirrup percentage ranged from 0.40 % to 2.56 %, the yielding stress of longitudinal reinforcement ranged from 314 MPa to 560 MPa, the yielding stress of stirrups ranged from 320 MPa to 672 MPa. The experimental database consists of a total of 76 tests given in details in the Table A.1. Beams are identified

using the notations in the first row, with the first letter of researchers' name. The same series of test was used before by several authors. Tang (2006) developed a radial basis function neural networks to predict the ultimate torsional strength of RC beams, Zhang (2002) and Hossain et al. (2006) improved analytical methods for predicting the nonlinear response of RC beams by using the same database. (Cevik et al.,2010)

Table 5.1 Ranges of variables of the database

	Minimum	Maximum	Increment
x (mm)	160	350	Variable
y (mm)	275	508	Variable
x ₁ (mm)	130	300	Variable
y ₁ (mm)	216	469	Variable
f _c (MPa)	26	110	Variable
s (mm)	50	215	Variable
A _t (mm ²)	71	127	Variable
f _{yv} (MPa)	319	672	Variable
A _l (mm ²)	381	3438	Variable
f _{yl} (MPa)	310	638	Variable
ρ _t (%)	0.22	2.56	Variable
ρ _l (%)	0.30	3.51	Variable

Related parameters of the GP training are presented in Table 5.2. Statistical parameters of the proposed GP models with the formulations are given in Table 5.3. The performance of GP model vs. test results is shown in Figure 5.1. As seen from Table 5.3 the best formulation was Equation 5.1. Afterwards, The entire database with corresponding experimental and GP Results of Equation 5.1 are given in Table A.1. The expression tree of the GP models is presented in Figure 5.2(a) the final formulation for the best torsional strength formulation of RC beams is obtained as follows:

$$T_u = (\sqrt[5]{A_L f_{yL}} - A_c) \cdot (\sqrt[5]{A_t f_{yt} / s / A_c / P_c}) \cdot (\sqrt[5]{A_c} - 8.26) \cdot \sqrt[2]{f_c / 0.085} \cdot \sqrt[2]{\sqrt[3]{A_L f_{yL}}} \quad (5.1)$$

Table 5.2 Parameters of GP model

<i>P1</i>	Function Set	+ , - , * , / , $\sqrt{\quad}$, ln
<i>P2</i>	Chromosomes	30-200
<i>P3</i>	Head Size:	2-6
<i>P4</i>	Number of Genes:	1-4
<i>P5</i>	Linking Function:	Addition, Multiplication
<i>P6</i>	Fitness Function Error Type:	MAE, RMSE, Custom Function
<i>P7</i>	Mutation Rate:	0,044
<i>P8</i>	Inversion Rate:	0,1
<i>P9</i>	One-Point Recombination Rate:	0,3
<i>P10</i>	Two-Point Recombination Rate:	0,3
<i>P11</i>	Gene Recombination Rate:	0,1
<i>P12</i>	Gene Transposition Rate:	0,1

Table 5.3 Statistical parameters of the proposed GP models with the formulations

Model	GP Formulation	Testing Set			Training Set			Total Set		
		R2	Mean	COV	R2	Mean	COV	R2	Mean	COV
1	$T_u = (\sqrt[5]{A_L f_{yL}} - A_c) \cdot (\sqrt[5]{A_t f_{yt}/s / A_c / P_c}) \cdot (\sqrt[5]{A_c} - 8.26) \cdot \sqrt[2]{f_c / 0.085} \cdot \sqrt[3]{A_L f_{yL}} \quad (5.1)$	0.969	0.942	0.18	0.961	0.99	0.21	0.958	0.99	0.20
2	$T_u = (3.36 \times 10^{-4}) \cdot (\sqrt[3]{A_c} + f_c) \cdot \sqrt[3]{A_L f_{yL}} - A_c \cdot (2.55 \times 10^{-4}) \cdot ((-3.22 x f_c^2) + A_c) \quad (5.2)$	0.942	1.28	0.66	0.940	1.03	0.26	0.922	1.08	0.44
3	$T_u = (3.31 \times 10^{-8}) \cdot \sqrt[4]{\sqrt[2]{\sqrt[2]{A_L f_{yL}} \cdot ((A_t f_{yt}/s) + (P_c / 1.82)) \cdot (A_c - (2x A_t f_{yt}/s)) \cdot \sqrt{(A_L f_{yL} / 9.98 / P_c), P_c}} \quad (5.3)$ <p>if $A_L f_{yL} / 9.98 / P_c \leq P_c$ result = $A_L f_{yL} / 9.98 / P_c$ else result = P_c</p>	0.962	0.99	0.21	0.941	1.02	0.28	0.945	1.01	0.26

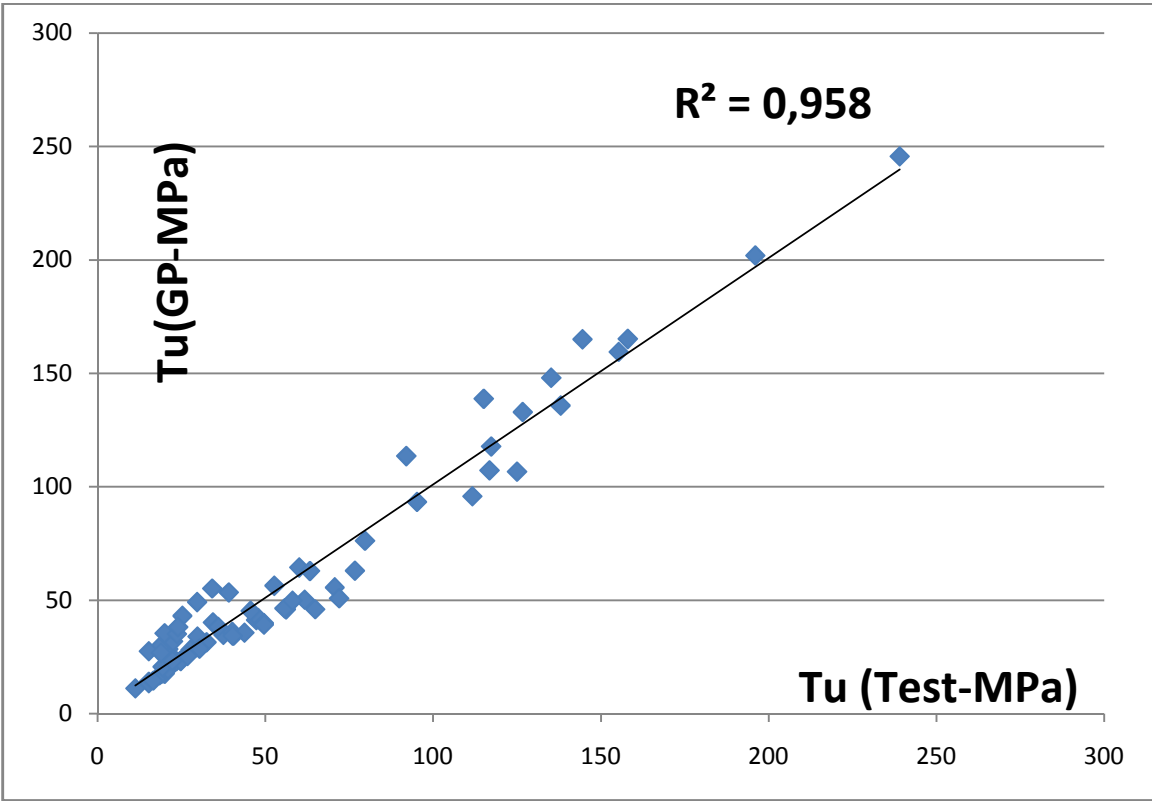
In order to investigate the accuracy of standards for torsional strength, the test results given in Table 5.4 were compared with the approaches of mentioned building codes. The predicting capability of codes related to torsional strength of the beams for mentioned tested 76 specimens are presented in Table 5.4. (Cevik et al.,2010)

Table 5.4. Prediction Accuracy of existing building codes

Building Standards	Expression for torsional strength	R ² (%)
ACI-318-2005	$T_n = \frac{2A_o A_t f_{yv}}{s} \cot \theta$	85.93
BS8110	$T_n = \frac{0.8x_1 y_1 (0.87f_{ys}) A_{sv}}{s}$	81.76
TBC-500-2000	$T_n = \frac{2A_e A_e f_{yv}}{2(x_1 + y_1)}$	71.07
AS3600	$T_n = \frac{2A_o A_t f_{yv}}{s} \cot \theta$	85.93
Eurocode-2-01	$T_n = f_{ys} (A_{sw} / s) 2A_k \cot \theta$	73.44
Eurocode-2-02	$T_n = f_y (A_s / u_k) 2A_k \tan \theta$	85.93
Eurocode-2-03	$T_n = 1.2(1 - f_{ck} / 250) f_{ck} A_k t_{ef} \sin \theta \cos \theta$	61.88
CSA	$T_n = \frac{2A_o A_t f_{yv}}{s} \cot \theta$	85.93
GP Model-1		96
GP Model-2		92
GP Model-3		95

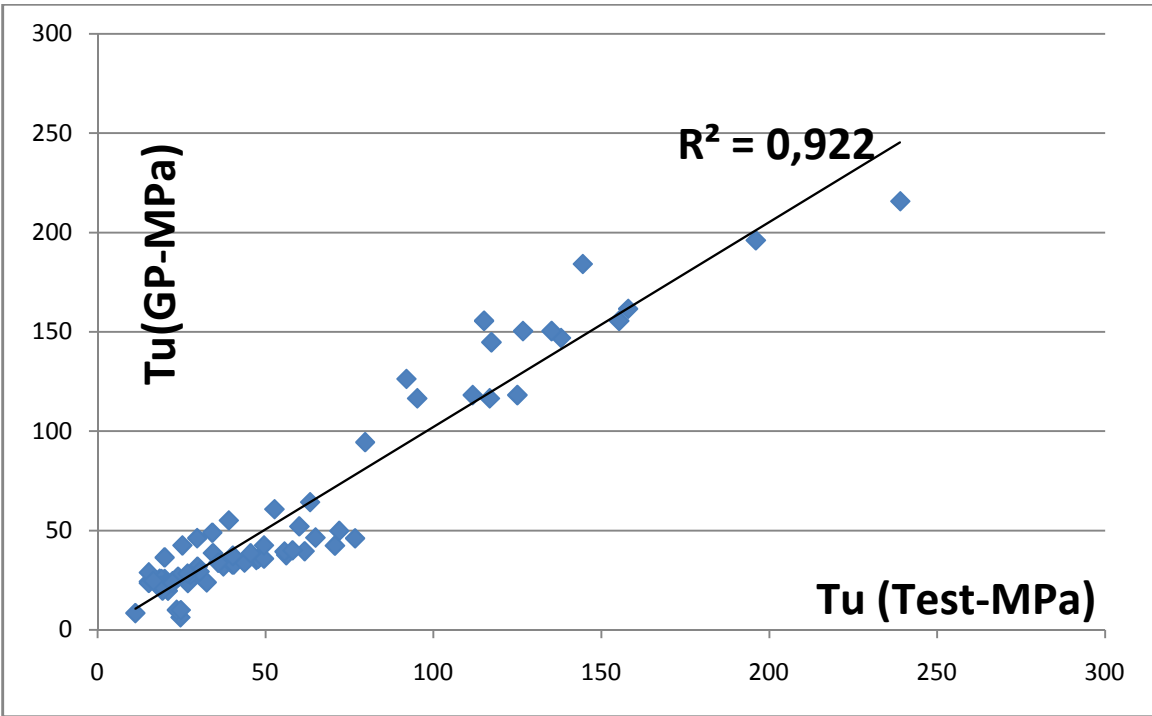
The performance of the proposed GP models vs. experimental results are given in Figure 5.1.

Model-1



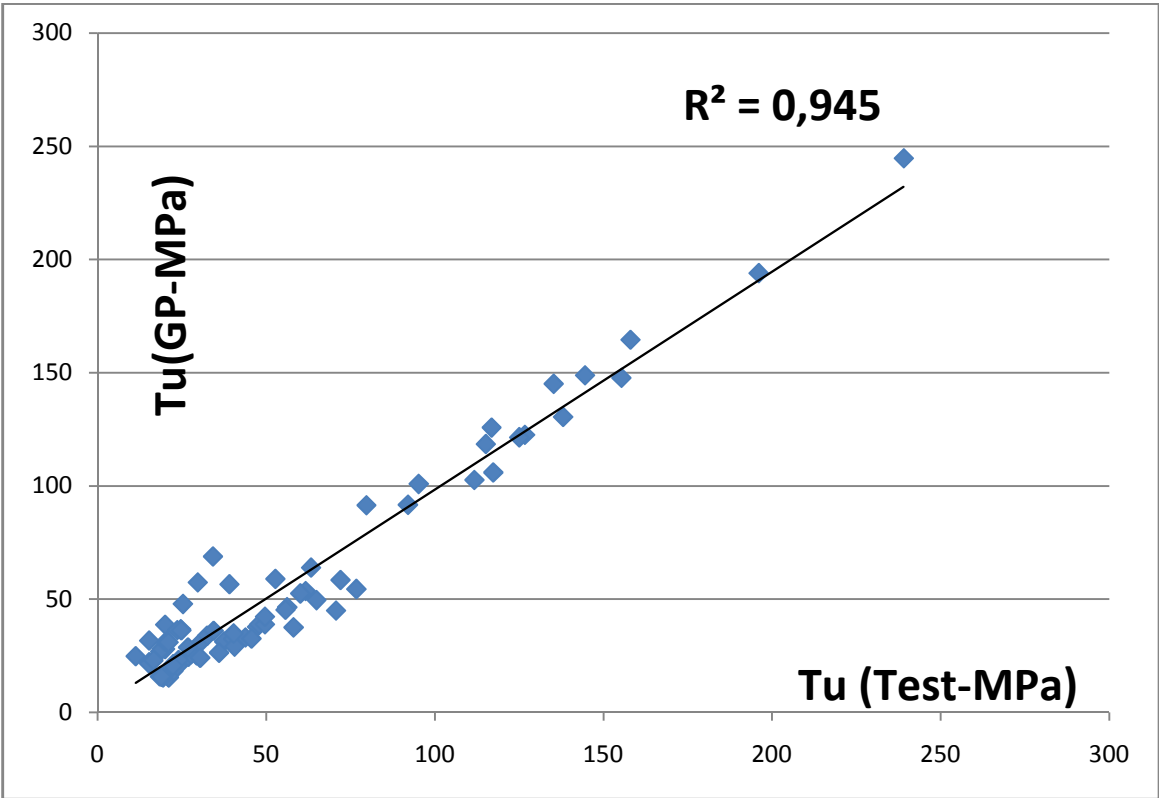
(a)

Model-2



(b)

Model-3

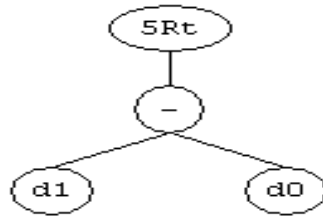


(c)

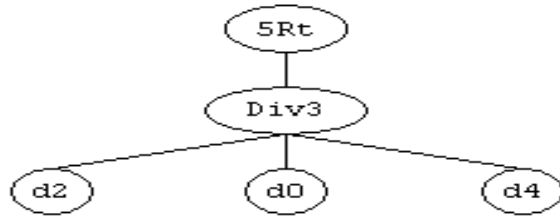
Figure 5.1(a),(b) and (c). Performance of Test and GP Results

Model-1

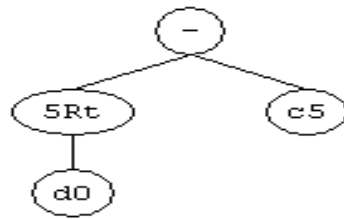
Sub-ET 1



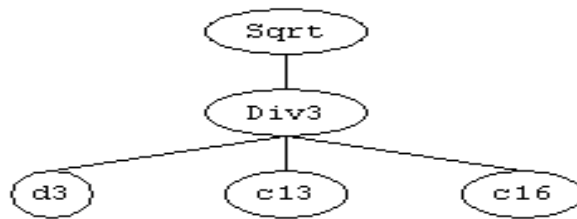
Sub-ET 2



Sub-ET 3



Sub-ET 4



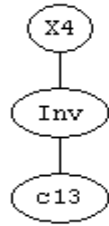
Sub-ET 5



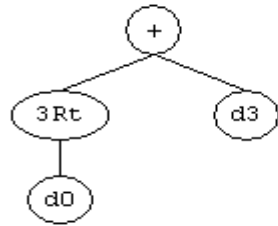
(a)

Model-2

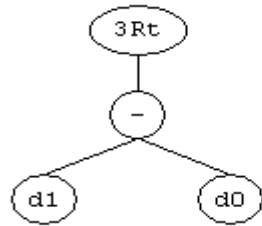
Sub-ET 1



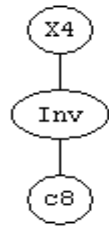
Sub-ET 2



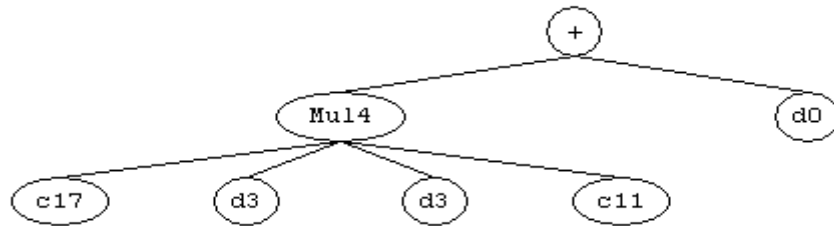
Sub-ET 3



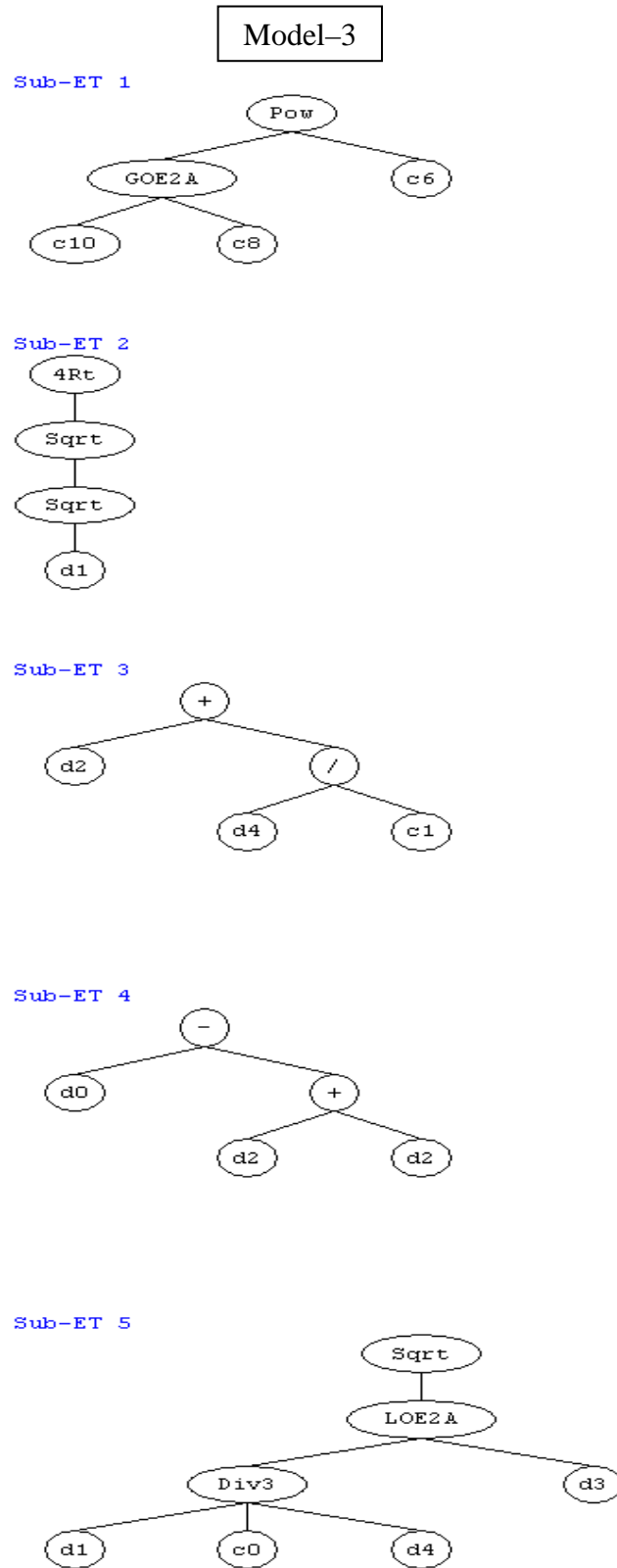
Sub-ET 4



Sub-ET 5



(b)



(c)

Figure 5.2(a),(b) and (c) Expression Tree for Torsional Strength of RC beams

5.2 Discussions

5.2.1 Code Approaches

The prediction accuracy of various standards of building codes related to torsional strength of the beams for mentioned tested 76 specimens are presented in Table 4. As seen from Table 4, ACI-318-2005 (2005), AS3600 (2005) and CSA (1994) torsional strength expressions have the most powerful estimating capacity. The differences between the codes and test results are based on some reasons such as;

- In all codes except for Eurocode-2-03 approaches given in Equation $T_n = 1.2(1 - f_c / 250)f_c A_k t_{ef} \sin\theta \cos\theta$, the concrete contribution is ignored after torsional cracking that makes no distinction between the behavior of normal and high strength concretes. Therefore, there is no advantage in using higher concrete strength in resisting ultimate torsion. However, the test series have shown that the ultimate torsional strength of RC beams increases with the increase of concrete quality.
- In the calculation of torsional strength, the main parameter is the shear flow area determined differently in the building codes. Taking the centers of longitudinal bars or centre-to-centre of stirrups for this calculation create a considerable difference in the total result.
- The building codes assume the longitudinal bars and stirrups to be yielded. But in the experiment that represents the real conditions more realist than analytical approaches, neither longitudinal bars nor stirrups yielded or either longitudinal bars or stirrups yielded. Especially high values of yield stresses, larger sizes of reinforcement and weaker concrete gives way the dominance of the neither longitudinal bars nor stirrups yielded.
- In the TBC-500-2000 (2000) and BS8110 (1985), the angle of cracks are neglected (or assumed 45°). This assumption induces the important differences between the code approaches and test results.

- The theoretical values computed by using code formulations are generally higher than the experimental torsional strength. This can be explained probably by the fact that the thin-walled tube and space truss analogy deviate in the particular and isolated case of overreinforced beams with low concrete strength.
- The comparison suggests that the most equations overestimate the strength, especially in the case of beams with low concrete strength. This is expected since most of the methods do not taking account the concrete strength in calculating the torsional strength. (Cevik et al.,2010)

5.2.2 Genetic Programming (GP)

Based on the findings of the GP the following comparisons can be drawn;

- The results of the proposed GP formulation performed better than building code's results.
- The error between the test and GP model is quite small for mentioned parameters. However, in the comparison of the code and test data, especially for over reinforced concrete, the predicting capability of code has become less.
- According to the final formulation for torsional strength, the ultimate torsional strength T_u of RC beams under pure torsion can be fairly accurately estimated using only five input variables x_1 , y_1 , f_c , A_1 and ρ_t (i.e. short dimension of the closed stirrup, long dimension of the closed stirrup, concrete compressive strength, longitudinal torsional reinforcement and steel ratio of stirrups).
- The outcomes of GP offer original contributions beside its high estimation capacity. (Cevik et al.,2010)

5.3 Main Effects of Variables on Torsional Strength

The main effect plot is an important graphical tool to visualize the independent impact of each variable on torsional strength. This graphical tool enables a better and simple picture of the overall importance of variable effects on the output which is the torsional strength. The slope of the line for each variable the degree of its effect on the output. To obtain the main effect plot a wide range of parametric study has been performed by using the proposed GP model. From main effect plot in Figure 5.3 it can be concluded that all variables used for GP modeling given in the experimental database have significant effects on torsional strength. (Cevik et al.,2010) Variables that are observed to be directly proportional from Figure 5.2 are A_c , P_c , f_c , $A_l f_{yl}$, $A_t f_{yt}/s$, ρ_t and ρ_l . The evaluation of separate interaction effects plot between any two variables is also performed shown in details in Figure 5.4 also the interaction graphs in 3D format are presented in Figures 5.5-5.14.

Main Effects Plot for Tu Data Means

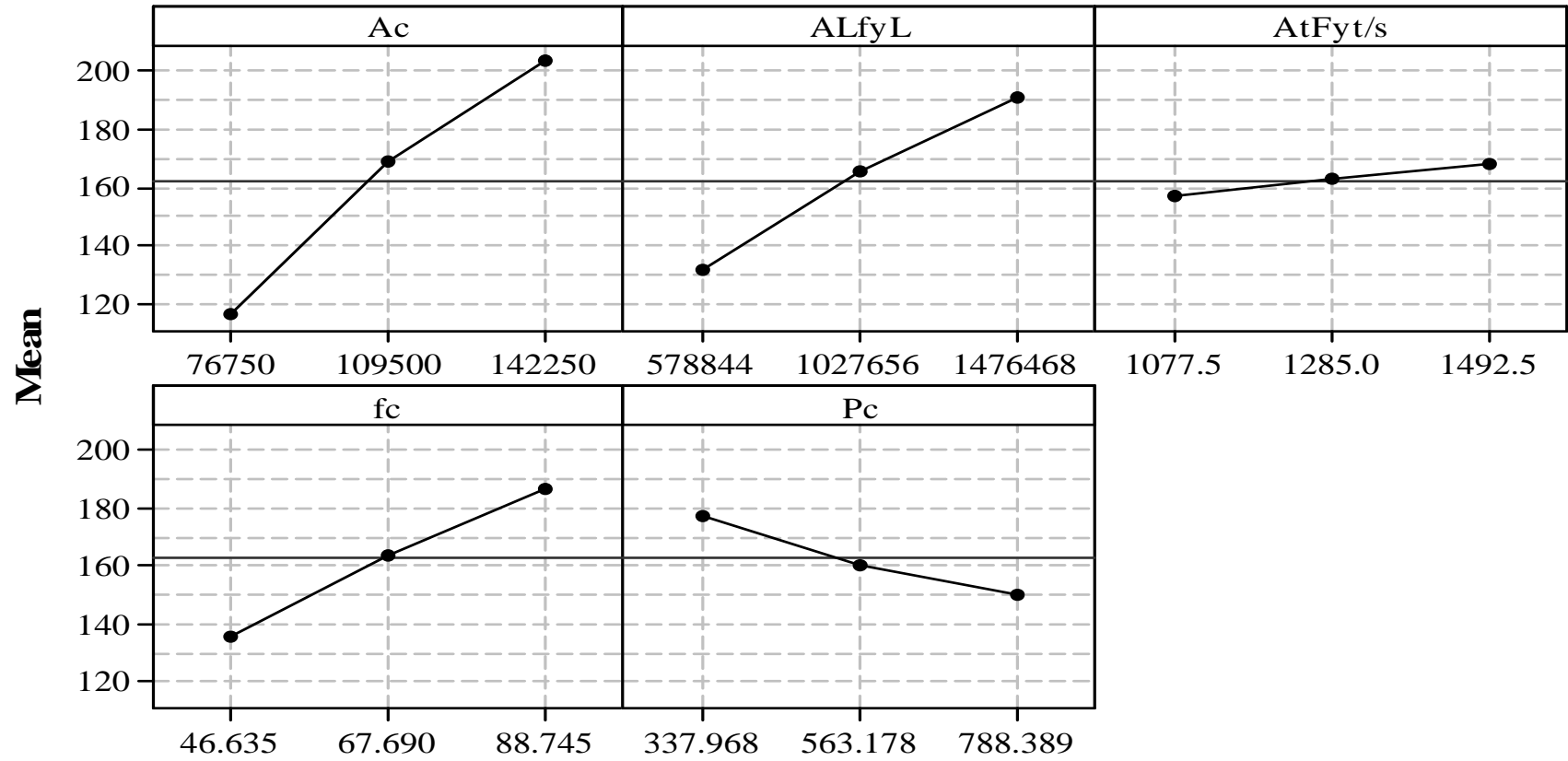


Figure 5.3 Main Effect Plot for Tu

Interaction Plot for Tu Data Means

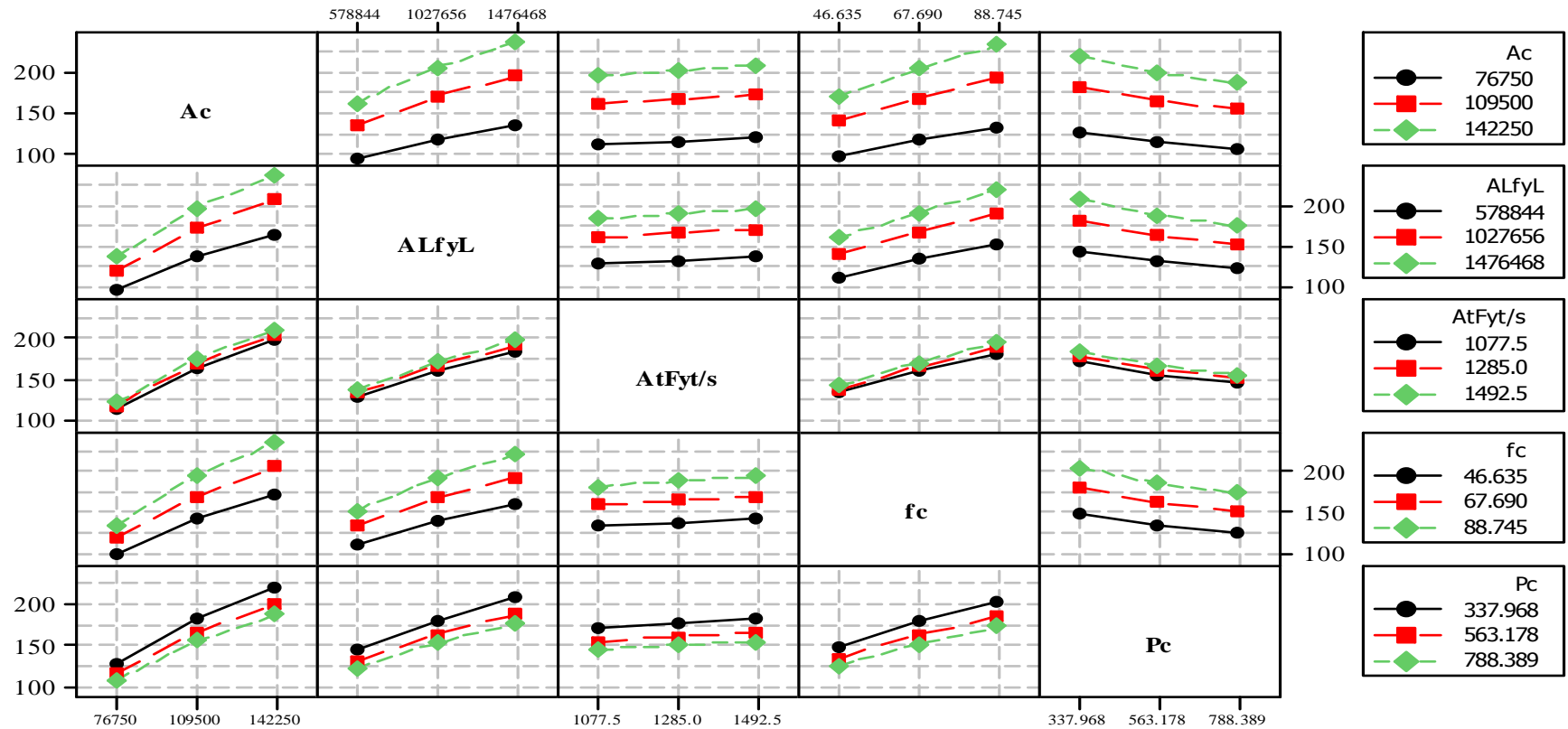


Figure 5.4 Interaction Plot for Tu

Surface Plot of Tu vs Ac, ALfyL

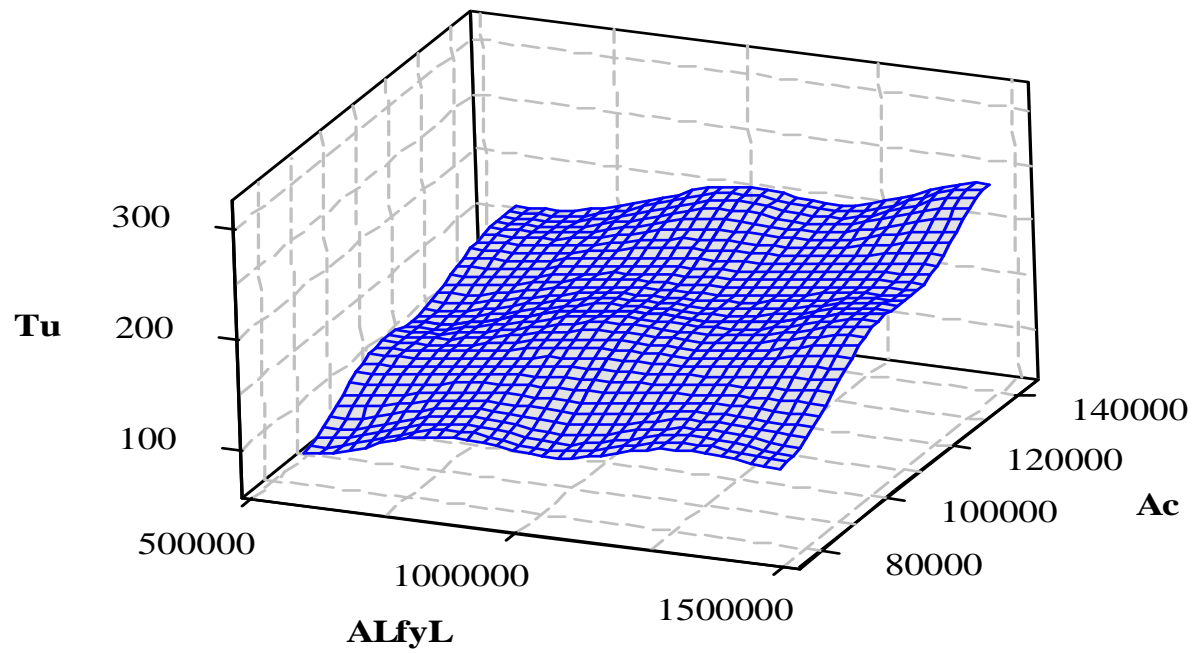


Figure 5.5 Surface Plot of Tu vs Ac, ALfyL

Surface Plot of Tu vs Ac, AtFyt/s

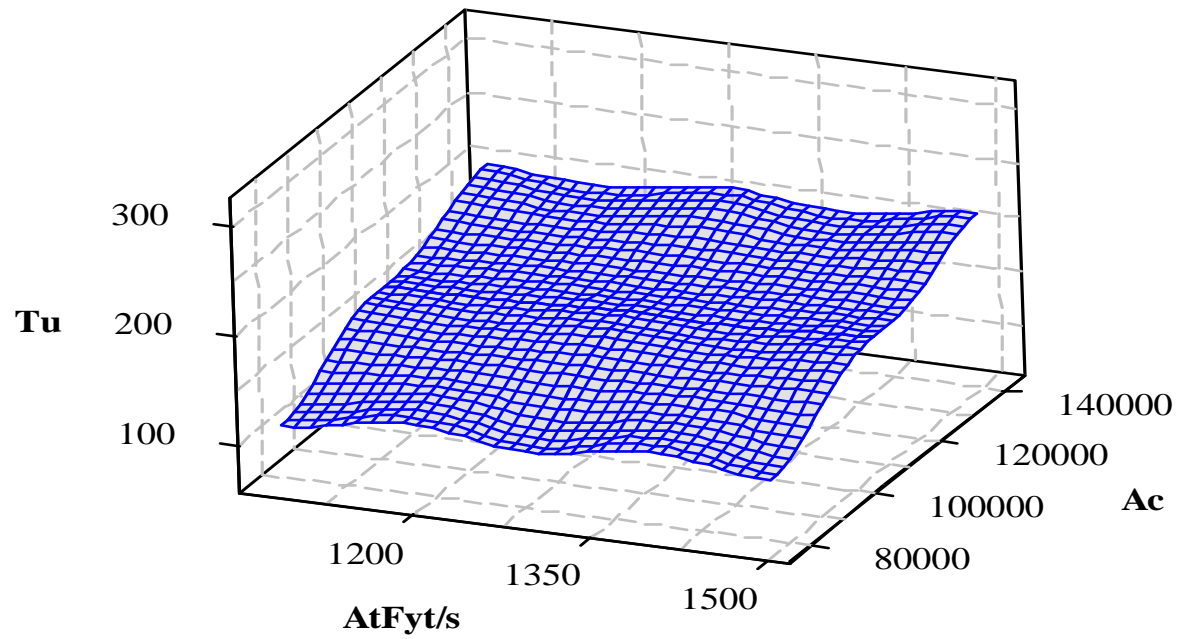


Figure 5.6 Surface Plot of Tu vs Ac, $A_{t,fyt/s}$

Surface Plot of Tu vs Ac, fc

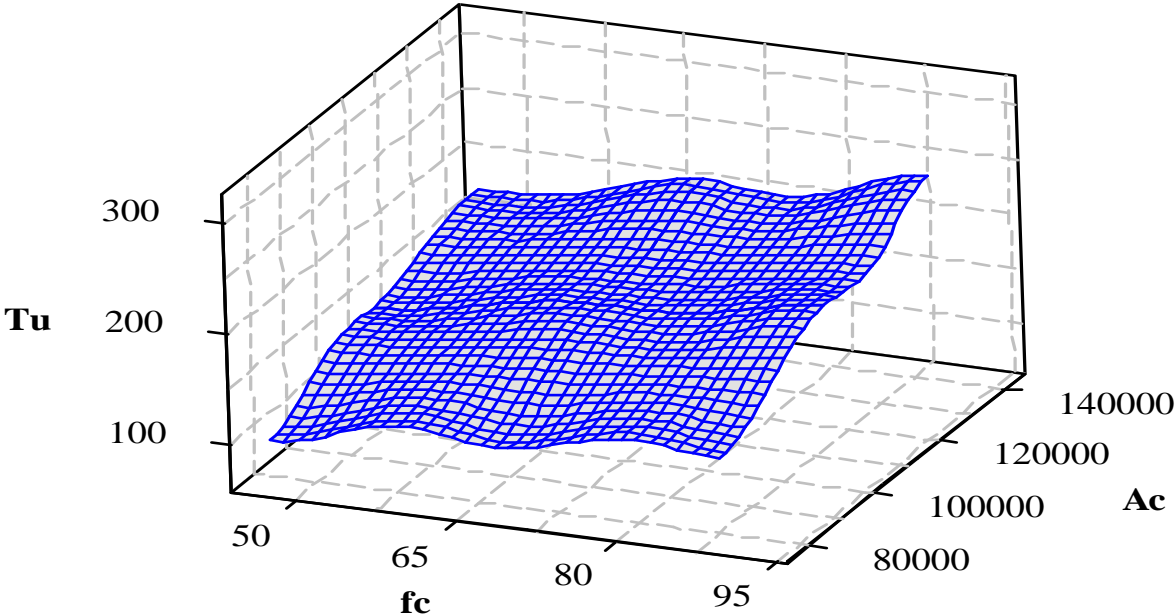


Figure 5.7 Surface Plot of Tu vs Ac, fc

Surface Plot of Tu vs Ac, Pc

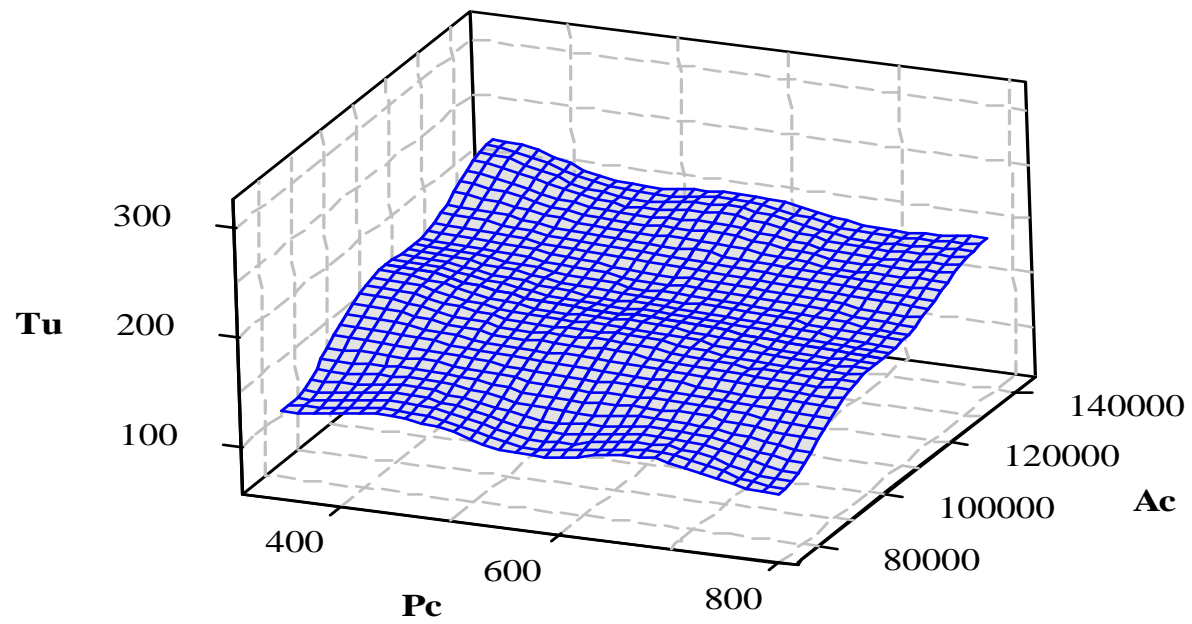


Figure 5.8 Surface Plot of Tu vs Ac, Pc

Surface Plot of Tu vs ALfyL, Pc

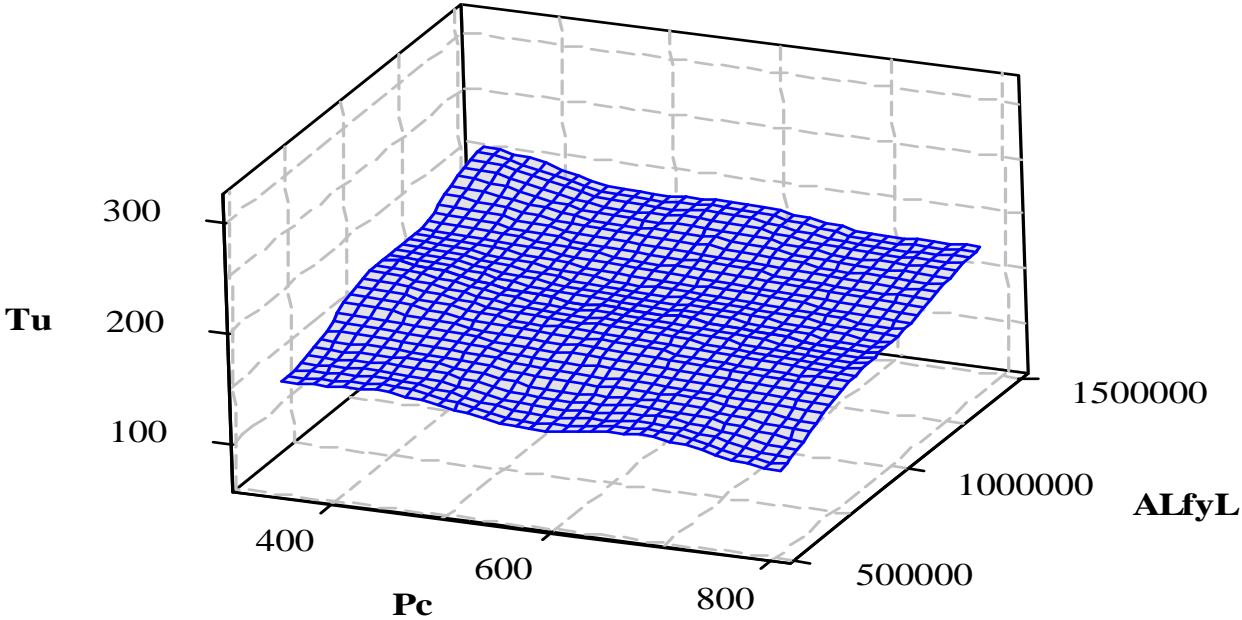


Figure 5.9 Surface Plot of Tu vs ALfyL, Pc

Surface Plot of Tu vs ALfyL, fc

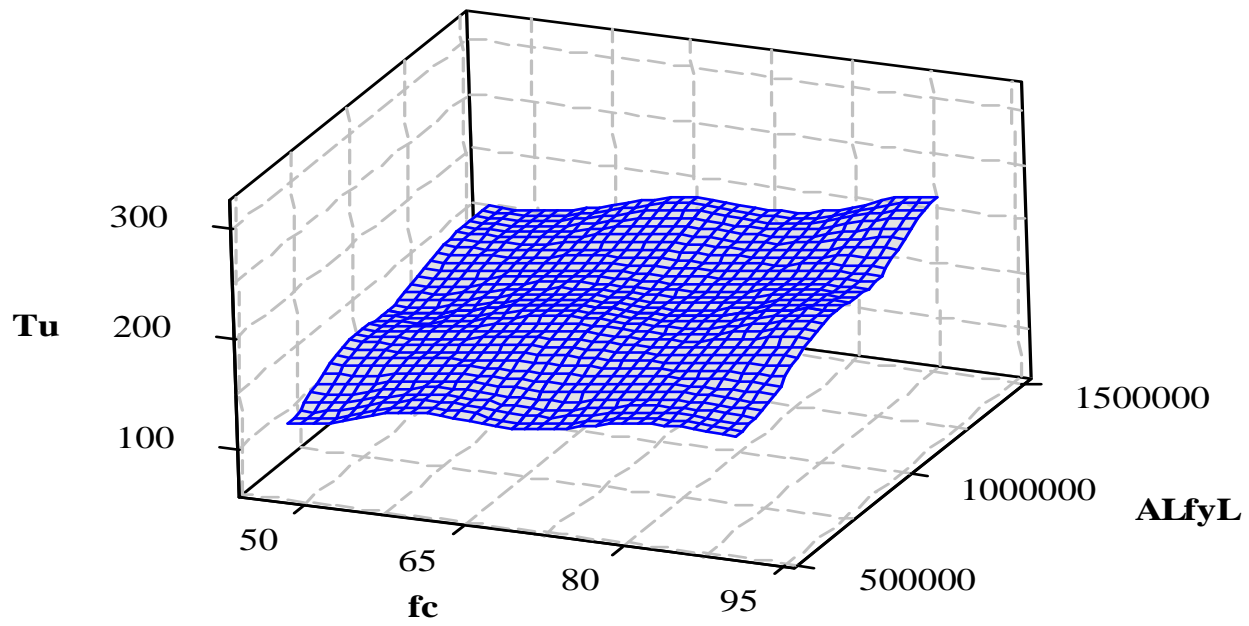


Figure 5.10 Surface Plot of Tu vs ALfyL,fc

Surface Plot of Tu vs ALfyL, AtFyt/s

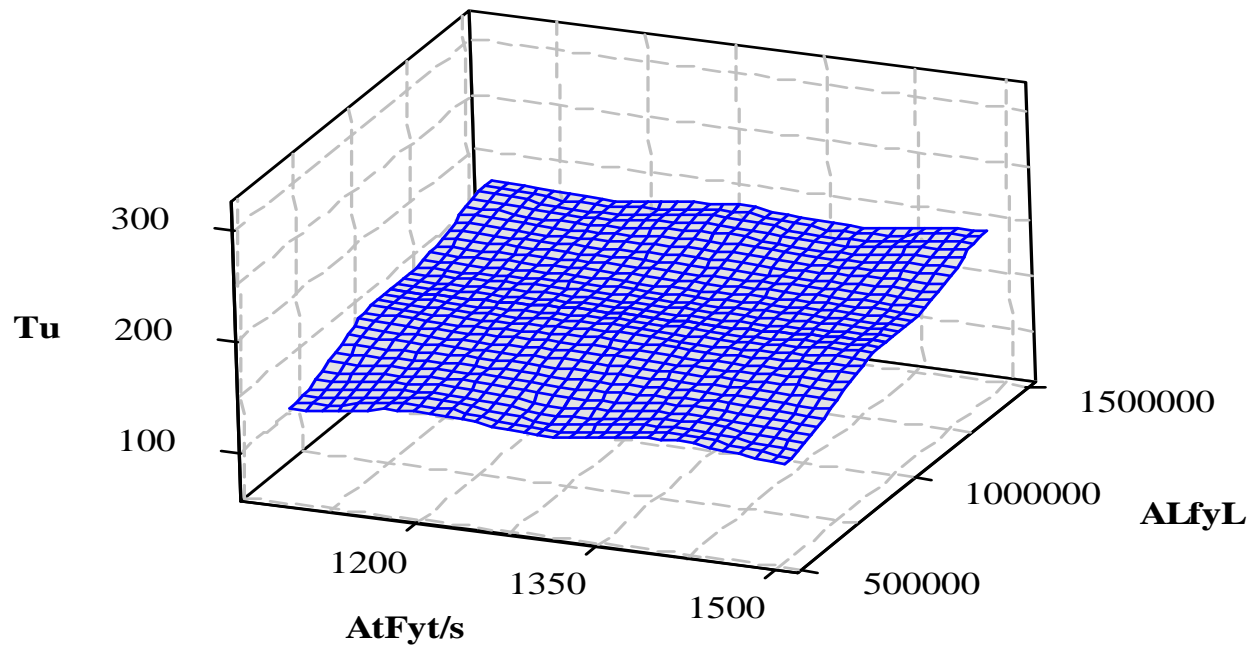


Figure 5.11 Surface Plot of Tu vs $A_L f_{yL}$, $A_t f_{yt}/s$

Surface Plot of T_u vs $A_t F_{yt}/s, f_c$

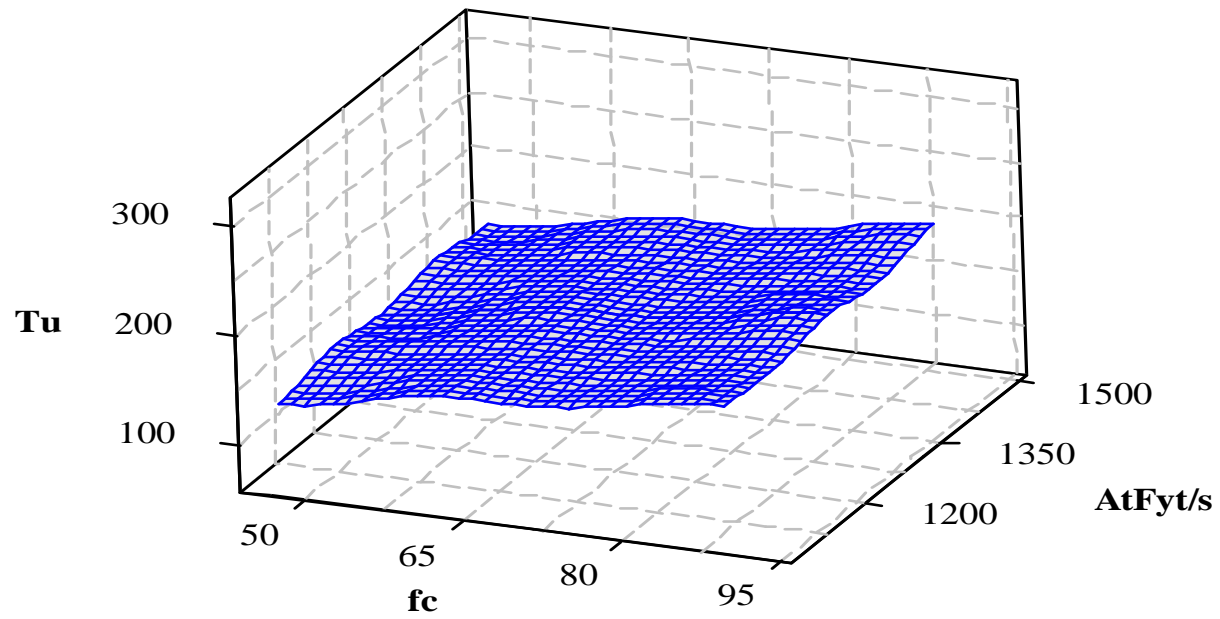


Figure 5.12 Surface Plot of T_u vs, $A_t f_{yt}/s, f_c$

Surface Plot of Tu vs AtFyt/s, Pc

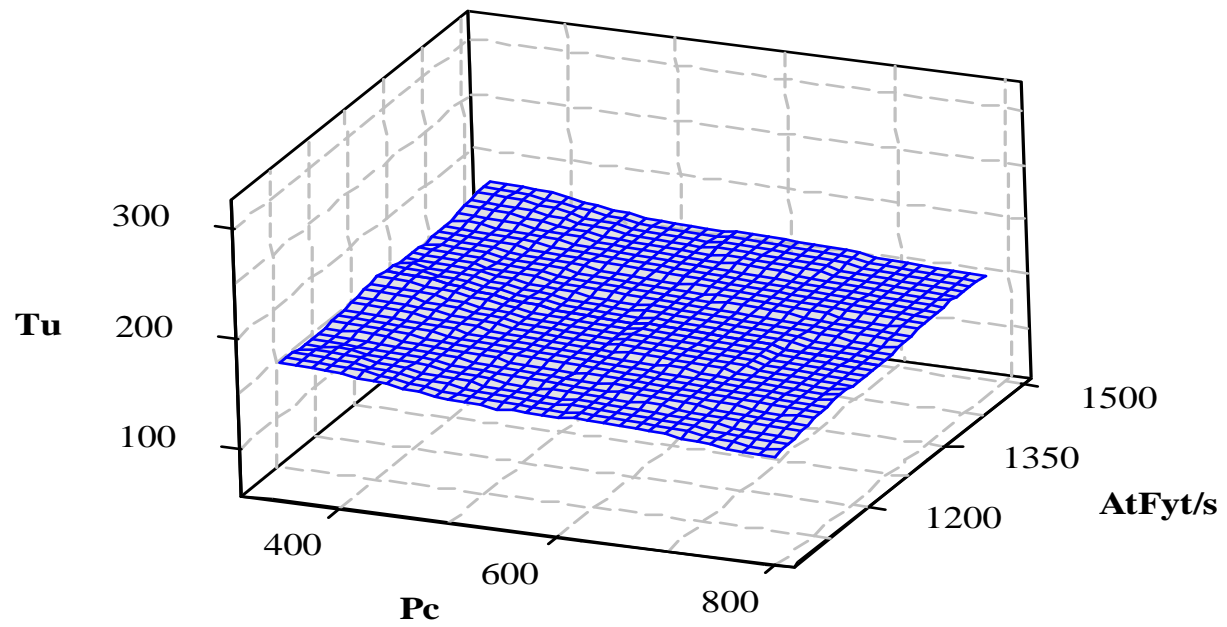


Figure 5.13 Surface Plot of T_u vs, $A_t f_{yt}/s, P_c$

Surface Plot of Tu vs fc, Pc

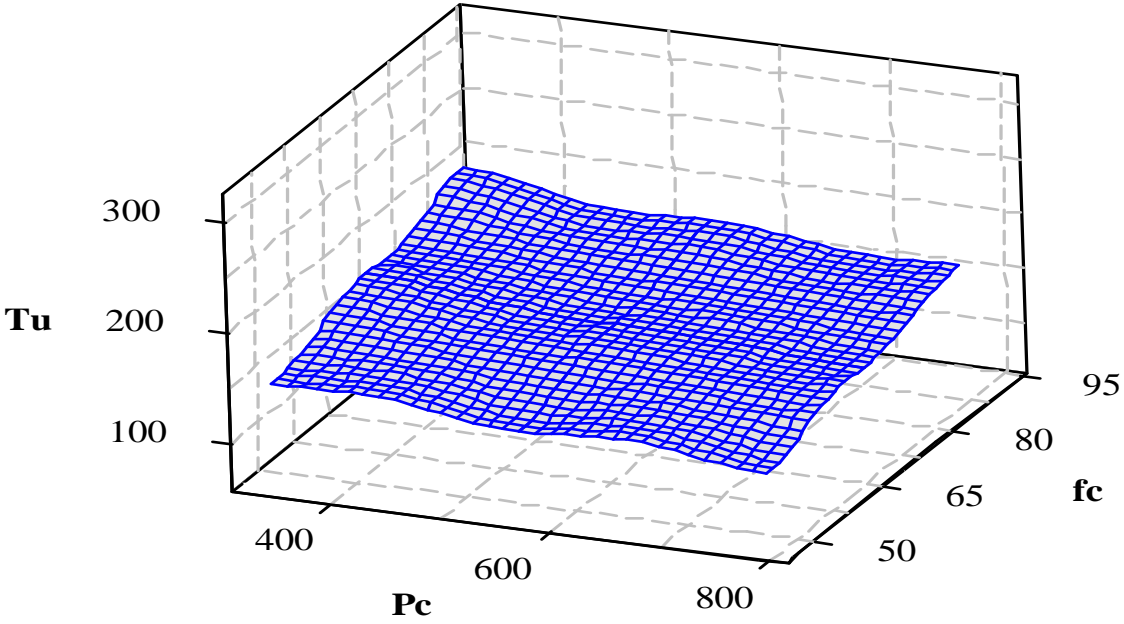


Figure 5.14 Surface Plot of Tu vs fc, Pc

CHAPTER 6

CONCLUSION

6.1 Conclusion

This study is a pioneer work that addresses the feasibility of GP as an alternative approach for the empirical formulation of torsional strength of RC beams for the first time. The use of ANN provides an alternative way to estimate torsional strength of RC beams. The proposed GP model is based on a wide range experimental database collected from the literature. The results of the proposed GP model are seen to be by far more accurate than current design codes and existing equations available in literature. Most of the design codes and equations available in literature are based on the regression analysis of predefined functions. However in the case of GP approach presented in this study, there is no predefined function to be considered. The GP approach generates various formulations and optimizes the best one that fits the experimental database best. The outcomes of this study are quite satisfactory which may serve GP approaches to widely used in further applications in the field of reinforced concrete structures.

APPENDIX

Table A1. Experimental Database (Rasmussen,1995),(Koutchoukali,2001),(Fang,2004),(Hsu,1968)

No	A_c	P_c	f_c	$A_{Lf_{yL}}$	$A_{tf_{yt}/s}$	Tu (Test)	Tu (GP)	Tu(GP)/ Tu(Test)
FS-1	175000	1700	78,5	526504	313,852	92	113,52	1,23
F2-2	175000	1700	78,5	831152	313,852	115,1	138,78	1,21
FS-3	175000	1700	78,5	831152	627,704	155,3	159,42	1,03
FS-4	175000	1700	78,5	1489800	627,704	196	201,91	1,03
FS-5	175000	1700	78,5	1925280	1013,600	239	245,58	1,03
FS-6	175000	1700	68,4	859500	332,873	126,7	132,94	1,05
FS-7	175000	1700	68,4	859500	570,150	135,2	148,04	1,09
FS-8	175000	1700	68,4	1432500	348,724	144,5	165	1,14
FS-9	175000	1700	35,5	524304	313,852	79,7	76,19	0,96
FS-10	175000	1700	35,5	831152	313,852	95,2	93,33	0,98
FS-11	175000	1700	35,5	831152	627,704	116,8	107,21	0,92
FS-12	175000	1700	35,5	1489800	627,704	138	135,78	0,98
FS-13	175000	1700	35,5	1925280	1013,600	158	165,15	1,05
FS-14	175000	1700	35,5	859500	332,873	111,7	95,77	0,86
FS-15	175000	1700	35,5	859500	570,150	125	106,65	0,85

FS-16	175000	1700	35,5	1432500	332,873	117,3	117,77	1
KB-1	61915	1016	39,6	195624,8	246,353	19,4	20,68	1,07
KB-2	61915	1016	64,6	195624,8	263,525	18,9	26,77	1,42
KB-3	61915	1016	75	195624,8	246,353	21,1	28,46	1,35
KB-4	61915	1016	80,6	195624,8	263,525	19,4	29,9	1,54
KB-5	61915	1016	93,9	195624,8	254,939	21	32,06	1,53
KB-6	61915	1016	76,2	195624,8	269,935	18,4	29,22	1,59
KB-7	61915	1016	72,9	242248,58	289,825	22,5	31,89	1,42
KB-8	61915	1016	75,9	283554,6	305,926	23,7	35,19	1,48
KB-9	61915	1016	76,7	301872	393,334	24	38,19	1,59
RB-1	44000	870	41,7	957218	580,323	16,6	14,55	0,88
RB-2	44000	870	38,2	985008,2	583,814	15,3	14,09	0,92
RB-3	44000	870	36,3	934059,5	586,432	15,3	13,47	0,88
RB-4	44000	870	61,8	944866,8	580,323	20	17,62	0,88
RB-5	44000	870	57,1	947954,6	580,323	18,5	16,96	0,92
RB-6	44000	870	61,7	944866,8	580,323	19,1	17,61	0,92
RB-7	44000	870	77,3	952586,3	574,215	20,1	19,73	0,98
RB-8	44000	870	76,9	947954,6	572,469	20,7	19,63	0,95
RB-9	44000	870	76,2	952586,3	578,578	21	19,61	0,93
RB-10	44000	870	109,8	943562,4	571,597	24,7	23,4	0,95
RB-11	44000	870	105	967991,2	575,960	23,6	23,14	0,98
RB-12	44000	870	105,1	971113,1	571,597	24,8	23,15	0,93

HS-1	96774	1270	27,58	159364,68	159,739	22,3	23,31	1,05
HS-2	96774	1270	28,61	200958,45	223,820	29,3	29,23	1
HS-3	96774	1270	28,06	249555	319,164	37,5	34,79	0,93
HS-4	96774	1270	30,54	284408,88	444,632	47,3	41,3	0,87
HS-5	96774	1270	29,03	337647,28	582,385	56,2	45,97	0,82
HS-6	96774	1270	28,82	379064,52	714,725	61,7	50,21	0,81
HS-7	96774	1270	25,99	162519,36	317,788	26,9	26,31	0,98
HS-8	96774	1270	26,75	163570,92	708,634	32,5	31,47	0,97
HS-9	96774	1270	28,82	243253,26	284,884	29,8	34,03	1,14
HS-10	96774	1270	26,48	382219,2	284,310	34,4	40,17	1,17
HS-11	96774	1270	26,61	169174,16	158,124	22,4	23,76	1,06
HS-12	96774	1270	25,58	204895,45	231,537	27,7	28,13	1,02
HS-13	96774	1270	28,41	260352,54	332,233	40,2	36,02	0,9
HS-14	96774	1270	30,61	293601,14	457,632	47,9	42,2	0,88
HS-15	96774	1270	29,85	207086,2	168,542	30,4	28,68	0,94
HS-16	96774	1270	30,54	250606,56	242,855	40,6	34,43	0,85
HS-17	96774	1270	26,75	286249,11	295,772	43,8	35,73	0,82
HS-18	96774	1270	26,54	323636,64	394,727	49,6	39,89	0,8
HS-19	96774	1270	27,99	383007,87	507,644	55,7	46,42	0,83
HS-20	96774	1270	29,37	727240,8	617,368	60,1	64,44	1,07
HS-21	96774	1270	45,23	206648,05	252,382	36	38,23	1,06
HS-22	96774	1270	44,75	261640,32	332,922	45,6	45,34	0,99

HS-23	96774	1270	44,95	280115,01	448,150	58,1	49,82	0,86
HS-24	96774	1270	45,02	315224,16	589,871	70,7	55,63	0,79
HS-25	96774	1270	45,78	371966,49	728,481	76,7	63	0,82
HS-26	129032	1524	29,79	163570,92	129,048	26,8	25,47	0,95
HS-27	129032	1524	30,89	204895,45	197,212	40,3	34,3	0,85
HS-28	129032	1524	26,82	257959,86	266,501	49,6	39,22	0,79
HS-29	129032	1524	28,27	289307,27	379,080	64,9	46	0,71
HS-30	129032	1524	26,89	336245,2	483,053	72	50,83	0,71
HS-31	129032	1524	29,92	382553,6	348,734	39,1	53,44	1,37
HS-32	129032	1524	30,96	456498,9	279,824	52,7	56,39	1,07
HS-33	129032	1524	28,34	552534,84	397,227	63,3	62,89	0,99
HS-34	129032	1524	27,03	130031,49	112,757	11,3	11,19	0,99
HS-35	129032	1524	26,54	169875,2	209,101	15,3	27,55	1,8
HS-36	129032	1524	26,89	210153,25	298,901	20	35,4	1,77
HS-37	129032	1524	27,17	256382,52	420,834	25,3	43,1	1,7
HS-38	129032	1524	27,23	291760,91	569,250	29,7	49,19	1,66
HS-39	129032	1524	27,58	320832,48	766,992	34,2	55,17	1,61

FS : Fang(2004)

KB : Koutchoukali(2001)

RB : Rasmussen(1995)

HS : Hsu(1968)

Table A2. Training and Testing Results

TRAINING RESULTS		
Target	Model	Residual
155,3	159,4204926	4,120492607
196	201,9093576	5,90935762
239	245,5779351	6,577935134
126,7	132,9362921	6,236292135
79,7	76,19171847	3,508281534
95,2	93,32918982	1,87081018
116,8	107,2070868	9,592913181
138	135,7799972	2,220002849
158	165,1462405	7,1462405
111,7	95,77004399	15,92995601
125	106,6526649	18,34733507
21,1	28,4599833	7,359983298
19,4	29,90365977	10,50365977
21	32,06361609	11,06361609
18,4	29,21607738	10,81607738
22,5	31,8888648	9,388864797
15,3	14,08941762	1,210582377
15,3	13,4748585	1,825141499
20	17,62124526	2,378754744
18,5	16,95874766	1,541252343
19,1	17,60698281	1,493017187
20,1	19,72618184	0,373818156
20,7	19,62706373	1,072936272
21	19,61499935	1,385000654
29,3	29,23231646	6,77E-02
37,5	34,7857233	2,714276703
47,3	41,29530005	6,004699952
56,2	45,96704481	10,23295519
61,7	50,21256076	11,48743924
26,9	26,30876639	0,591233615
32,5	31,467436	1,032563997
29,8	34,02710275	4,227102747
34,4	40,1716983	5,7716983
22,4	23,76138646	1,361386457
27,7	28,12709652	0,427096519

40,2	36,02267222	4,177327777
47,9	42,20438585	5,695614146
30,4	28,67982932	1,720170679
40,6	34,4317016	6,168298404
43,8	35,73007914	8,069920859
49,6	39,89496248	9,705037515
55,7	46,41996686	9,280033142
60,1	64,4395312	4,339531199
36	38,22863207	2,228632071
45,6	45,33721888	0,262781125
58,1	49,81998124	8,280018755
70,7	55,63831538	15,06168462
49,6	39,22190644	10,37809356
64,9	46,00168344	18,89831656
72	50,83372388	21,16627612
39,1	53,44365718	14,34365718
52,7	56,39176039	3,691760389
63,3	62,89318551	0,406814493
11,3	11,18957281	0,110427186
15,3	27,5485534	12,2485534
20	35,39826669	15,39826669
25,3	43,10357655	17,80357655
29,7	49,19035481	19,49035481
34,2	55,17000146	20,97000146

TESTING RESULTS		
Target	Model	Residual
92	113,5211671	21,52116708
115,1	138,7835996	23,68359964
135,2	148,042219	12,84221896
144,5	165,0007576	20,50075761
117,3	117,7691083	0,469108301
19,4	20,68005084	1,280050842
18,9	26,77152316	7,871523158
23,7	35,18863839	11,48863839
24	38,18883289	14,18883289
16,6	14,54565245	2,054347546
24,7	23,40462074	1,295379263
23,6	23,14371396	0,456286039
24,8	23,14756319	1,652436815
22,3	23,31091604	1,010916043
76,7	63,00556173	13,69443827
26,8	25,46614689	1,333853113
40,3	34,30223625	5,997763754

REFERENCES

ACI Committee 318-71.(1971).*Building code requirements for structural concrete and commentary*. American Concrete Institute, Detroit.

ACI Committee 318-89 .(1989).*Building code requirements for structural concrete and commentary*. American Concrete Institute, Detroit.

ACI Committee 318-95.(1995).*Building code requirements for structural concrete and commentary*. American Concrete Institute, Detroit.

ACI Committee 318-99 .(1999). *Building code requirements for reinforced concreated*.

ACI Committee 318-2005.(2005).*Building Code Requirements for Structural Concrete(ACI318-05) and Commentary (318R-05)*. American Concrete Institute, Farmington Hills,Mich.

Ahmad, S. H., and Lue, D. M. (1987), Flexure-Shear Interaction of Reinforced High-Strength Concrete Beams, *ACI Structural Journal*, Vol. 84, No. 4, July-August, pp. 330-341.

Ahmad, S. H., Xie, Y., and Yu, T. (1994), Shear Strength of Reinforced Lightweight Concrete Beams of Normal and High Strength Concrete, *Magazine of Concrete Research*, Vol. 46, No. 166, March, pp. 57-66.

Ahmad, S. H., Park, F., and El-Dash, K. (1995), Web Reinforcement Effects on Shear Capacity of Reinforced High-Strength Concrete Beams, *Magazine of Concrete Research*, Vol. 47, No. 172, pp. 227-233.

Ahmad, S. H., Khaloo, A. R., and Poveda, A. (1986), Shear Capacity of Reinforced High-Strength Concrete Beams, *ACI Journal, Proceedings*, Vol. 83, No. 2, March-April, pp. 297-305.

Al-Alusi, A. F. (1957), Diagonal Tension Strength of Reinforced Concrete T-Beams with Varying Shear Span, *ACI Journal Proceedings*, Vol. 53, May, pp. 1067-1077.

AS3600 (2001) Concrete Structures, Standarts Association of Australia.

Bazant, Z. P., and Kazemi, M. T. (1991), Size Effect on Diagonal Shear Failure of Beams Without Stirrups, *ACI Structural Journal*, Vol. 88, No. 3, pp. 268-276.

Bresler, B., and Scordelis, A. C. (1963), Shear Strength of Reinforced Concrete Beams, *ACI Journal, Proceedings*, Vol. 60, No. 1, January, pp. 51-74.

BS8110 (1985). Structural Use of Concrete-Part 2. British Standards.

Canadian Standard Association (1994). Design of Concrete Structures: Structure Design. CSA Standard, A23-3-94, Canadian Standard Association, Rexdale, Ontario.

Candida F.(2001), Gene Expression Programming: Mathematical Modeling by an Artificial Intelligence.

Chambers L.(2001), The Practical Handbook of Genetic Algorithms Applications, 2nd Ed., Chapman & Hall/CRC.

Chao-Wei Tang (2006). Using Radial Basis Function Neural Networks to Model Torsion Strength of Reinforced Concrete Beams. *Computers and Concrete*, **3**, 335-355.

Çevik A., Arslan M.H., and Koroğlu M.A. (2010), Genetic Programming Based Modeling of Torsional Strength of RC Beams. *KSCE Journal of Civil Engineering*, **14**, 371-384.

Çevik A.(2007), A New Formulation for Longitudinally Stiffened Webs Subjected to Patch Loading, *Journal of Constructional Steel Research*, **63**, 1328-1340

Çevik A.(2007), A New Formulation for Web Crippling Strength of Cold-Formed Steel Sheeting Using Genetic programming, *Journal of Constructional Steel Research*, **63**, 867-883.

Çevik A.(2007), Genetic Programming Based Formulation of Rotation Capacity of Wide Flange Beams, *Journal of Constructional Steel Research*, **63**, 884-893.

Çevik A., Tohumoglu G., Canseven A.G., and Seyhan N.(2007), Formulation of ELF Magnetic Fields' Effects on Malondialdehyde Level and Myeloperoxidase Activity in Kidney Using Genetic Programming, *Computer Methods and Programs in Biomedicine*, **86**, 1-9.

Çevik A.(2008), Unified Formulation for Ultimate Capacity of Shear Failure of Arc Spot Welding Using Genetic Programming, *Journal of Materials Processing Technology*, **204**,117-124.

Çevik A. and Çabalar A.F.(2008), A Genetic-Programming-Based Formulation for the Strength Enhancement of Fiber-Reinforced-Polymer-Confined Concrete Cylinders, *Journal of Applied Polymer Science*, **110**, 3087-3095.

Çevik A. and Sonebi M.(2008), Modelling the performance of self-compacting SIFCON of cement slurries using genetic programming technique, *Computers and Concrete*, **5**, 475-490.

Çabalar A.F. and Çevik A.(2009), Genetic Programming-Based Attenuation Relationship: An Application of Recent Earthquakes in Turkey, *Computers & Geosciences*, **35**, 1884-1896.

Çevik A. and Çabalar A.F.(2009), Modelling Damping Ratio and Shear Modulus of Sand-Mica Mixtures Using Genetic Programming, *Expert Systems with Applications*, **36**, 7749-7757.

Sonebi M. and Çevik A.(2009), Genetic Programming Based Formulation for Fresh and Hardened Properties of Self-Compacting Concrete Containing Pulverised Fuel Ash, *Construction and Building Materials*, **23**, 2614-2622.

Çabalar A.F., Çevik A. and Güzelbey I.H.(2010), Constitutive Modeling of Leighton Buzzard Sands Using Genetic Programming, *Neural Computing & Applications*, **19**, 657-665.

Çevik A., Arslan M.H. and Koroğlu M.A.(2010), Genetic-Programming-Based Modeling of RC Beam Torsional Strength, *KSCE Journal of Civil Engineering*, **14**, 371-384.

Tanyildizi H. and Çevik A.(2010), Modeling Mechanical Performance of Lightweight Concrete Containing Silica Fume Exposed to High Temperature Using Genetic Programming, *Construction and Building Materials*, **24**, 2612-2618.

Koroğlu M.A., Köken A., Arslan M.H., and Çevik A.(2011), Genetic Programming Based Modeling of Shear Capacity of Composite Beams with Profiled Steel Sheeting, *Advanced Steel Construction*, **7**, 2

Dereli G.M.(2011), *Neural Network Modelling of Torsional Strength of RC Beams*
Gaziantep University

Edward G.Nawy.(2005).*Reinforced Concrete A Fundamental Approach*.(5th ed).
Prentice Hall International Series. William J. Hall Editor.

Ersoy U., Özcebe G., Tankut T.(2003) *Reinforced Concrete* Middle East Technical
University, Ankara

Elfegren L, Karlsson I, Losberg A. (1974), Torsion bending-shear interaction for concrete beams. *Journal of Structural Division ASCE*, **100**, 1657-1676

European Standard. Eurocode 2(2002), *Design of Concrete Structures*, Draft for Stage 49, Commission of the European Communities, European Committee for Standardization.

Fang IK. and Shiau JK., (2004).“Torsional Behavior of Normal and High Strength Concrete Beams” *ACI Structural Journal*,**101**, 304-313.

Ferreira C.(2001), Gene Expression Programming: A New Adaptive Algorithm for Solving Problems. *Complex Systems*, **13:2**, 87-129

Ferreira C(2001), Gene Expression Programming in Problem Solving, Invited Tutorial of the 6th Online World Conference on Soft Computing in Industrial Applications, September 10-24.

Goldberg,D.E.(1989). *Genetic Algorithms in Search, Optimization, and Machine Learning*.Reading, MA: Addison-Wesley.

Haupt RL, Haupt SE(2004), *Practical Genetic Algorithms*, 2nd Edition, Wiley-Interscience.

Holland, J. H.(1975), *Adaptation in Natural and Artificial Systems*. Ann Arbor: University of Michigan Press.

Hsu TTC.(1968), Torsion of Structural Concrete-Behavior of Reinforced Concrete Rectangular Members.Torsion of Structural Concrete SP-18, ACI, Farmington Hills. Mich.261-306.

Hsu TTC.(1968), Ultimate Torque of Reinforced Concrete Members. *Journal of the Structural Division*, ASCE,**94**, 485-510

Hsu, T. T. C. (1983) *Torsion of Reinforced Concrete*, Van Nostrand Reinhold, New York, 510 .

Hsu, T. T. C. (1990), Shear Flow Zone in Torsion of Reinforced Concrete, *Journal of the Structural Division, ASCE*, **116**, New York, November 3206 - 3225.

Hsu, T. T. C.(1993) *Unified Theory of Reinforced Concrete*. CRC Press. Boca Raton, FL.,313 .

Ireland JC, Baeten M, Foster J, Lutton E, Ryan C.(2002) Genetic Programming,5th European Conference, EuroGP.

Koutchoukali NE. and Belarbi G., (2001) Torsion of High Strength Reinforced Concrete Beams and Minimum Reinforcement Requirement *ACI Structural Journal* ,**98**, 462-469.

Koza JR, Keane MA, Streeter MJ, Mydlowec W, Yu J, Lanza G(2003), Genetic Programming IV: Routine Human-Competitive Machine Intelligence, Springer Verlag.

Lessig, N.N. (1953). *Theoretical and experimental investigations of reinforced concrete elements subjected to combined bending and torsion*. Theory of design and construction of reinforced concrete structures, 73-84.

Lessig N.N. (1959).Determination of carrying capacity of reinforced concrete elements with rectangular cross –section subjected to flexure with torsion *Zhelezonabetona*,**5**,:5-28.

Nawy, E. G.(2000). *High Performance Concrete*. (2nd ed). John Wiley & Sons. NewYork. 550 .

Nawy EG. (2003).*Reinforced concrete, a fundamental approach*, Pearson Education.

Rasmussen LJ, Baker G.(1995) Torsion in reinforced normal and high strength concrete beams part-I: An experimental test series. *ACI Structural Journal*; V.92, No.1: 56-62.

Tang CW.(2006), Using radial basis function neural networks to model torsional strength of reinforced concrete beams. *Computers and Concrete*; V.3, No.5: 335-355.

TBC-500 (2000): *Requirements for Design and Construction of Reinforced Concrete Structures*, Turkish Standards TS-500.

www.gepsoft.com

<http://www.gp-field-guide.org.uk/>

Yan W.(2003) “*Profitable, Return Enhancing*” *Portfolio Adjustments – An Application of Genetic Programming with Constrained Syntactic Structure*.

Zang Y. (2002), *Torsion in High Strength Concrete Rectangular Beams*, Master thesis, University of Nevada

